# Organometallic Pnicogen Complexes. VI. Synthesis, Structure, and Bonding of a New Iron–Antimony Cluster Complex, $\{[Fe(h^5\text{-}C_5H_5)(CO)_2]_3SbCl\}_2[FeCl_4]\cdot CH_2Cl_2$; Geometry of the Tetrachloroferrate(II) Anion and Its Stereochemical Relationship with Other Tetrachlorometalate Anions[1]

**Trinh-Toan and Lawrence F. Dahl***

*Contribution from the Department of Chemistry, University of Wisconsin, Madison, Wisconsin 53706.* *Received August 12, 1970*

**Abstract:** A new kind of antimony–(transition metal) cluster system has been isolated as a cation of the dark reddish purple crystalline salt $\{[Fe(h^5\text{-}C_5H_5)(CO)_2]_3SbCl\}_2[FeCl_4]\cdot CH_2Cl_2$ by the reaction of $Na[Fe(h^5\text{-}C_5H_5)(CO)_2]$ with $SbCl_3$. The characterization of this trimetal-substituted derivative of the nonisolatable tetrachlorostibonium cation was achieved from a three-dimensional X-ray diffraction analysis. Crystalline $\{[Fe(h^5\text{-}C_5H_5)(CO)_2]_3SbCl\}_2[FeCl_4]\cdot CH_2Cl_2$ is constructed of discrete $\{[Fe(h^5\text{-}C_5H_5)(CO)_2]_3SbCl\}^+$ cations, $[FeCl_4]^{2-}$ anions, and $CH_2Cl_2$ solvent molecules. In the cation the one chlorine and three $[Fe(h^5\text{-}C_5H_5)(CO)_2]$ ligands are markedly distorted from a regular tetrahedral arrangement about the central antimony atom; the orientations of two of the three $[Fe(h^5\text{-}C_5H_5)(CO)_2]$ ligands approximately conform to threefold symmetry about the Sb–Cl bond, with the disposition of the third one differing from this pseudothreefold geometry primarily by a rotation of approximately 143° about its Fe–Sb axis coupled with a small but significant angular distortion of the $Fe_3SbCl$ fragment from an idealized $C_{3v}$-3$m$ geometry to an experimentally observed $C_s$-$m$ one. The hitherto unknown Fe–Sb bond length is of average value 2.54 Å, while the Sb–Cl bond length is 2.401 (4) Å. A detailed comparison of the stereochemical features of this cation with those of electronically equivalent, neutral tin–(transition metal) cluster molecules is made, including a discussion of the nature of the Sb–Cl and Sb–Fe bonding. The structural data of the $[FeCl_4]^{2-}$ anion (of crystallographic site symmetry $C_2$-2) are compared to those of the other tetrachlorometalate anions $[MCl_4]^{2-}$ (M = Mn, Co, Ni, Cu, Zn), and rationalizations of the observed trends in average M–Cl bond lengths in this series and in the $[FeCl_4]^-$–$[FeCl_4]^{2-}$ pair are made in terms of bonding arguments. The fact that the determined mean value of 2.30 Å for the Fe(II)–Cl bonds in the $[FeCl_4]^{2-}$ anion is 0.11–0.14 Å longer than the average values for Fe(III)–Cl lengths found in several salts containing $[FeCl_4]^-$ anions illustrates that the placement of the one extra electron of the $[FeCl_4]^{2-}$ anion in an antibonding MO (of doubly degenerate representation e under assumed cubic $T_d$-$\bar{4}3m$ symmetry) and the interdependent size expansion of the appropriate iron valence orbitals due to a less positive charge on the Fe(II) nucleus produce a drastic enlargement of the Fe–Cl bonds. The significant difference in the two crystallographically distinct Fe–Cl bond lengths of 2.284 (4) and 2.320 (5) Å in the $[FeCl_4]^{2-}$ anion together with its observed angular distortion are attributed in part to the interaction of two of the four chlorine atoms of the $[FeCl_4]^{2-}$ anion with the hydrogen atoms of the $CH_2Cl_2$ molecule. Crystalline $\{[Fe(h^5\text{-}C_5H_5)(CO)_2]_3SbCl\}_2[FeCl_4]\cdot CH_2Cl_2$ forms monoclinic crystals, with four formula species in a unit cell of centrosymmetric space group $I2/c$ and of dimensions $a$ = 19.360 (2), $b$ = 17.111 (1), $c$ = 16.850 (2) Å, and $\beta$ = 94.06 (1)°; the calculated and observed densities are 1.979 and 1.986 g/cm³, respectively. An anisotropic–isotropic full-matrix least-squares refinement of the nonhydrogen atoms yielded final discrepancy values of $R_1$ = 7.1 and $R_2$ = 6.4% for the 2040 independent data ($I \geq 2\sigma(I)$) collected with a Datex automated General Electric diffractometer.

Although a large number of transition metal cluster compounds containing tin atoms have been structurally characterized,[2-17] structures of (transition metal)–antimony cluster compounds are as yet unreported. Recent developments in our laboratories in the field of (transition metal)–arsenic cluster systems[18,19]

(1) (a) Previous paper in this series: A. S. Foust and L. F. Dahl, *J. Amer. Chem. Soc.*, **92**, 7337 (1970); (b) presented in part at the Inorganic Symposium on "Structure and Chemistry of Compounds with Metal-Metal Bonds," Joint Conference of the Chemical Institute of Canada and the American Chemical Society, Toronto, Canada, May 1970.

(2) B. T. Kilbourn and H. M. Powell, *Chem. Ind. (London)*, 1578 (1964).

(3) (a) R. D. Cramer, R. V. Lindsey, Jr., C. T. Prewitt, and U. G. Stolberg, *J. Amer. Chem. Soc.*, **87**, 658 (1965); (b) L. J. Guggenberger, *Chem. Commun.*, 512 (1968).

(4) J. D. Cotton, J. Duckworth, S. A. R. Knox, P. F. Lindley, I. Paul, F. G. A. Stone, and P. Woodward, *ibid.*, 253 (1966).

(5) H. P. Weber and R. F. Bryan, *ibid.*, 443 (1966); *Acta Crystallogr.*, 22, 822 (1967).

(6) (a) R. F. Bryan, *J. Chem. Soc. A*, 172 (1967); (b) *ibid.*, *A*, 192 (1967); (c) *Chem. Commun.*, 355 (1967).

(7) R. F. Bryan and A. R. Manning, *ibid.*, 1220 (1968).

(8) R. Mason, G. B. Robertson, P. O. Whimp, and D. A. White, *ibid.*, 1655 (1968).

(9) R. K. Pomeroy, M. Elder, D. Hall, and W. A. G. Graham, *ibid.*, 381 (1969).

(10) (a) B. P. Bir'yukov, Yu. T. Struchkov, K. N. Anisimov, N. E. Kolobova, O. P. Osipova, and M. Ya. Zakharov, *ibid.*, 749 (1967); (b) B. P. Bir'yukov, Yu. T. Struchkov, K. N. Anisimov, N. E. Kolobova, and V. V. Skripkin, *ibid.*, 750 (1967); (c) B. P. Bir'yukov, Yu. T. Struchkov, K. N. Anisimov, N. E. Kolobova, and V. V. Skripkin, *ibid.*, 159 (1968).

(11) R. M. Sweet, C. J. Fritchie, Jr., and R. A. Schunn, *Inorg. Chem.*, **6**, 749 (1967).

(12) J. E. O'Connor and E. R. Corey, *ibid.*, **6**, 968 (1967).

(13) J. E. O'Connor and E. R. Corey, *J. Amer. Chem. Soc.*, **89**, 3930 (1967).

(14) J. H. Tsai, J. J. Flynn, and F. P. Boer, *Chem. Commun.*, 702 (1967).

(15) P. F. Lindley and P. Woodward, *J. Chem. Soc. A*, 382 (1967).

(16) B. P. Bir'yukov and Yu. T. Struchkov, *Zh. Strukt. Khim.*, 10, 95 (1969); *Chem. Abstr.*, 70, 119131*d* (1969).

(17) R. F. Bryan, P. T. Greene, G. A. Melson, P. F. Stokely, and A. R. Manning, *Chem. Commun.*, 722 (1969).

(18) A. S. Foust, M. S. Foster, and L. F. Dahl, *J. Amer. Chem. Soc.*, **91**, 5631 (1969).

(19) A. S. Foust, M. S. Foster, and L. F. Dahl, *ibid.*, **91**, 5633 (1969).

prompted further investigations with the purpose of obtaining antimony homologs. These studies instead have led to the synthesis and characterization of new (transition metal)–antimony complexes which have included the cubane-type molecules $\{[Fe(h^5\text{-}C_5H_5)(CO)_2Cl][SbCl_3]\}_4$[20] and $Co_4(CO)_{12}Sb_4$.[1] The present paper reports the synthesis and structural characterization of the tetrachloroferrate(II) salt of the chlorotris(dicarbonyl-$\pi$-cyclopentadienyliron) stibonium cation, which is of prime interest and significance with regard to the stereochemistry of both the antimony–iron cluster cation and the anion.

## Experimental Section

**Preparation and Properties.** All reactions were performed in standard glass apparatus in an atmosphere of dry, prepurified nitrogen. All glassware was dried at 125° and flushed with nitrogen before use. THF (Matheson Coleman and Bell) was refluxed over calcium hydride overnight before distillation. Dichloromethane (Eastman Organic Chemicals) was used without further purification. The $[Fe(h^5\text{-}C_5H_5)(CO)_2]_2$ (Alfa Inorganics, Inc.) was recrystallized from a $CH_2Cl_2$–octane solution. $SbCl_3$ (Alfa Inorganics, Inc.) was purified by sublimation. A solution of $Na[Fe(h^5\text{-}C_5H_5)(CO)_2]$ was prepared after the method of Gorisch[21] from the reaction of 10.6 g (0.03 mol) of $[Fe(h^5\text{-}C_5H_5)(CO_2)]_2$ with sodium amalgam (3.0 g of Na and 300 g of Hg) in about 250 ml of THF. The mixture was stirred rapidly at room temperature for 24 hr to give an orange-brown solution. After the excess of amalgam was separated, a THF solution containing 4.6 g (0.02 mol) of $SbCl_3$ was introduced dropwise to the reaction mixture which was then stirred at room temperature for 24 hr. After the reaction was completed, the solvent was removed from the reaction mixture in a water-aspirator vacuum. A dark brown solid remained which was extracted with 100-ml portions of dichloromethane; the extracts then were filtered. The resulting residue consisted of some pyrophoric compounds which decomposed violently when exposed to air. Up to this stage, apparently the filtrate did not contain an appreciable amount of the chlorotriiron stibonium cation, because the salt itself is sparingly soluble in dichloromethane. An infrared spectrum of the filtrate showed several other absorption bands in the carbonyl stretching region in addition to those bands corresponding to $[Fe(h^5\text{-}C_5H_5)(CO)_2]_2$ (with its characteristic bridging carbonyl frequency at 1760 $cm^{-1}$) and the two very strong carbonyl bands at 2050 and 2010 $cm^{-1}$ of the $Fe(h^5\text{-}C_5H_5)(CO)_2Cl$ compound which was subsequently isolated.[20] Other products characterized were the starting $SbCl_3$ and the decomposition product, ferrocene. The filtrate was set in the dark at room temperature under an atmosphere of nitrogen for 30 days; at the end of this time 2.1 g of dark red-purple crystals of $\{[Fe(h^5\text{-}C_5H_5)(CO)_2]_3SbCl\}_2[FeCl_4]\cdot CH_2Cl_2$ was deposited on the walls of the flask.

From the insolubility of the salt in dichloromethane and the abundance of $Fe(h^5\text{-}C_5H_5)(CO)_2Cl$ in the reaction mixture, it is suggested that the cation was formed directly from the reaction of the latter compound with $SbCl_3$, a step similar to the formation of $[Fe(h^5\text{-}C_5H_5)(CO)_2Sb(C_6H_5)_3]^+$ cation.[22] However, the direct reaction of $Fe(h^5\text{-}C_5H_5)(CO)_2Cl$ with $SbCl_3$ failed under our conditions to give the desired cation.

The formation of the $[FeCl_4]^{2-}$ anion was a pleasant surprise. Tetrahalo complexes of Fe(II) are known to be easily oxidizable and difficult to recrystallize.[23] Fortunately, in an oxygen-free and strongly reduced medium (with Na/Hg starting material) the formation of $[FeCl_4]^{2-}$ from $Cl^-$ ions which exist in excess in the solution is favorable. The crystallization and stabilization of this anion apparently were made possible by the presence of the very bulky stibonium cations. *Anal.* Calcd for $C_{42}H_{30}O_{12}Cl_6Fe_7Sb_2\cdot CH_2Cl_2$: C, 31.14; H, 1.94; Cl, 17.10; Fe, 23.57. Found:[24] C, 30.50; H, 1.95; Cl, 16.36; Fe, 24.68. The ionic dark red-purple crystals are insoluble in nonpolar organic solvents but soluble in more polar ones such as acetonitrile, with some instantaneous decomposition. The solid, which is stable in air, decomposes at about 200° without melting.

**Infrared, Mass Spectrometric, and Proton Magnetic Resonance Data.** Infrared spectra were recorded on a Beckman IR-8 spectrometer. An infrared spectrum of the salt (in $CH_3CN$ solution) exhibited bands typical of terminal carbonyl stretching modes at 2050 (sh), 2025 (vs), and 1990 (s) $cm^{-1}$. Another infrared spectrum in solid form (KBr pellet) showed bands at 3280 (w), 3125 (w), 1415 (m), 850–860 (m, very broad), and 750 (m, broad) $cm^{-1}$, characteristic of metal-coordinated cyclopentadienyl groups, besides the multiplet at 2045 (s), 2020 (s), 2015 (sh), 1990 (s), and 1970 (s) $cm^{-1}$, characteristic of terminal carbonyl groups.

The mass spectrum of $\{[Fe(h^5\text{-}C_5H_5)(CO)_2]_3SbCl\}_2[FeCl_4]\cdot CH_2Cl_2$ was obtained from an AEI Model MS-902 mass spectrometer located at the University of Wisconsin.[25] In order to obtain the spectra for this ionic complex high-temperature conditions were used. Operating conditions were 70 eV of electron energy and a probe temperature of 200° with samples introduced into the ion source by a direct inlet system. Under these operating conditions the mass spectral data of $\{[Fe(h^5\text{-}C_5H_5)(CO)_2]_3SbCl\}_2[FeCl_4]\cdot CH_2Cl_2$, whose major $m/e$ peaks with their relative abundances are given in Table I for the cation, do not suggest an $Fe_3Sb$ cluster system. Not only is the parent peak corresponding to the cation containing three $[Fe(h^5\text{-}C_5H_5)(CO)_2]$ segments linked by Fe–Sb bonds to the central SbCl part absent, but also all peaks corresponding to any fragments containing the $Fe_3Sb$ cluster are missing. Instead the highest observed peak matches a cation with two $[Fe(h^5\text{-}C_5H_5)(CO)_2]$ segments attached to an SbCl part along with other peaks corresponding to various fragments of the $Fe_2Sb$ and FeSb clusters. This fragmentation pattern thereby illustrates that mass spectrometric results (especially those not obtained under a variety of operating conditions) may sometimes be misleading with respect to interpretation in terms of the compound's composition. In this particular instance, an X-ray diffraction study was required to ascertain the stoichiometry as well as atomic arrangement.

Table I. Mass Spectrum of $\{[Fe(h^5\text{-}C_5H_5)(CO)_2]_3SbCl\}_2[FeCl_4]\cdot CH_2Cl_2$

| Species | $m/e$[a] | Relative abundance[b] |
|---|---|---|
| $ClSbFe_2(C_5H_5)_2(CO)_4^+$ | 510 | 31 |
| $ClSbFe_2(C_5H_5)_2(CO)_2^+$ | 454 | 56 |
| $ClSbFe_2(C_5H_5)_2^+$ | 398 | 48 |
| $SbFe(C_5H_5)(CO)_2^+$ | 298 | 54 |
| $ClSbFe(C_5H_5)^+$ | 277 | 73 |
| $SbFe(C_5H_5)(CO)^+$ | 270 | 71 |
| $SbFe(C_5H_5)^+$ | 242 | 100 |
| $Fe(C_5H_5)_2^+$ | 186 | 590 |
| $Fe(C_5H_5)(CO)_2^+$ | 177 | 350 |
| $Fe(C_5H_5)Cl^+$ and $SbCl^+$ | 156 | 760 |
| $Fe(C_5H_5)^+$ | 121 | 760 |
| $Fe(C_3H_3)^+$ | 95 | 250 |
| $Fe(C_5H_5)^{2+}$ | 60.5 | 50 |
| $Fe^+$ | 56 | 1000 |
| $CO^+$ | 28 | 1300 |

[a] Listed $m/e$ values are based on $^{35}Cl$ and $^{121}Sb$. [b] Integrated for all isotopes.

Proton magnetic resonance spectra were obtained from a Varian Model A-60 spectrometer. The resonance of the cyclopentadienyl ring protons is not observed in the expected range because of the presence of the paramagnetic anion. All that is observed is the high-field shift of the methyl protons of $CH_3CN$ used as solvent.

Attempts to measure the magnetic susceptibility of the compound were unsuccessful. Correlation between the susceptibility and the solvent proton shift in the nmr spectrum could not be established because of the uncertainty in concentration due to partial decom-

(20) Trinh-Toan and L. F. Dahl, to be submitted for publication.
(21) R. D. Gorsich, *J. Amer. Chem. Soc.*, **84**, 2486 (1962).
(22) A. Davison, M. L. H. Green, and G. Wilkinson, *J. Chem. Soc.*, 3172 (1961).
(23) (a) C. Furlani, E. Cervone, and V. Valenti, *J. Inorg. Nucl. Chem.*, 25, 159 (1963); (b) N. S. Gill, *J. Chem. Soc.*, 3512 (1961); (c) C. D. Burbridge and D. M. L. Goodgame, *ibid.*, *A*, 1074 (1968).
(24) (a) Alfred Bernhardt Mikroanalytisches Laboratorium, 5251 Elbach über Engelskirchen, West Germany. (b) The small increase in percentage of iron and small decrease in the percentage of chlorine may reflect the partial loss of solvent molecule $CH_2Cl_2$ after the prolonged dryness under vacuum of the solvated salt, before being submitted for elemental analysis.
(25) We are indebted to Dr. A. S. Foust of the University of Wisconsin for running the mass spectra.

position of the unstable complex. Faraday magnetic measurements gave unusually high values of the magnetic susceptibility, apparently due to some ferromagnetic decomposition product on the surface of the crystals.

**Single-Crystal X-Ray Data.** Suitable single crystals were obtained in the manner described above. A regular cubic-shaped crystal of dimensions 0.18 (rotation axis) × 0.20 × 0.17 mm was mounted on a glass fiber with epoxy cement. Preliminary oscillation and Weissenberg photographs showed $C_{2h}$-2/*m* Laue symmetry characteristic of the monoclinic system. The crystal was first optically aligned about the rotation axis (corresponding to the monoclinic *c* axis, with *b* axis unique) and then centered in the X-ray beam of a General Electric four-circle automated diffractometer.[26] Twenty-one representative diffraction maxima were carefully centered, and with these angle settings, lattice and orientation parameters and instrument constants $2\theta_0$ and $\chi_0$ were calculated and refined by a procedure[27] which minimizes the distance between observed and calculated reciprocal lattice points. These constants and parameters were then used to generate the angle settings for all data reflections.[28] The collection and treatment of intensity data have been described previously.[29] All intensity data were collected by the $\theta$–$2\theta$ scan technique with symmetric $2\theta$ scans at 2.0°/min rate with stationary-crystal–stationary-counter background counts of 15 sec taken at the beginning and end of each scan. Intensity data ($hkl$, $\bar{h}kl$, $h\bar{k}l$, $hk\bar{l}$, $\bar{h}\bar{k}l$, $\bar{h}k\bar{l}$, $h\bar{k}\bar{l}$, $\bar{h}\bar{k}\bar{l}$) were collected for $2\theta \leq 40°$. In this case, because some of the peaks were broad, variable scan ranges for $2\theta$ were used: 3.0° for $5° \leq 2\theta \leq 10°$, 2.5° for $10° < 2\theta \leq 20°$, and 2.0° for $20° < 2\theta \leq 40°$.

The radiation used was Zr-filtered Mo K$\alpha$ ($\lambda$ 0.71069 Å). Three standard reflections were monitored after every 100 reflections in order to check electronic and crystal stability. During the entire collection of three independent data sets, the intensities of the standard reflections linearly decreased by only ~3% of their initial values; hence no corrections for crystal decay were made. Fifteen low-angle reflections had intensities which exceeded the linear limits of the pulse-height analyzer. Hence, measurements of these intensities were repeated with Zr-foil attenuators placed between the crystal and the counter. The proper scale factor necessary to merge these intensities with the other data was obtained by measurements with and without attentuation of the intensities of several sets of standard reflections. The intensities were corrected for background and Lorentz-polarization effects as previously described.[29] A given reflection was considered "unobserved" if I was less than $2\sigma(I)$. This procedure yielded a total of 2040 observed and 788 unobserved independent reflections (besides the sytematic absences required by the space group). The linear absorption coefficient,[30] $\mu$, for Mo K$\alpha$ radiation is 32.2 cm$^{-1}$. Based on this absorption coefficient together with the previously mentioned dimensions of the regularly shaped crystal, the calculated transmission coefficients ranged from only 0.38 to 0.43.[31] Since these extreme values of the absorption correction[31] caused only a ±2–3% fluctuation in $|F|$'s, absorption corrections were neglected. No extinction corrections were made.

The atomic scattering factors used for all atoms are those based on Hartree–Fock–Slater calculations as compiled by Hanson, *et al.*[32] Dispersion corrections for atomic scattering factors were made for antimony, iron, and chlorine atoms.[33]

**Unit Cell and Space Group.** The measured lattice constants (25°) and estimated standard deviations for the monoclinic unit cell of $\{[Fe(h^5\text{-}C_5H_5)CO)_2]_3SbCl\}_2[FeCl_4]\cdot CH_2Cl_2$ are $a$ = 19.360 (2), $b$ = 17.111 (1), $c$ = 16.850 (2) Å, $\beta$ = 94.06 (1)°; the volume of the unit cell is 5568 Å$^3$. The density of 1.979 g/cm$^3$ calculated on the basis of four of the above formula species per cell agrees well with the experimental value of 1.986 g/cm$^3$ measured by the flotation method with mixtures of 1,2-dibromoethane and 1,3-dibromopropane. The total number of electrons per unit cell, $F(000)$, is 3224.

Systematic absences of $\{hkl\}$ for $h + k + l = 2n + 1$ and $\{h0l\}$ for $l = 2n + 1$ imply either the space group *Ic* [nonstandard setting of *Cc* ($C_s^4$, no. 9), *b* axis unique] or *I*2/*c* [nonstandard setting of *C*2/*c* ($C_{2h}^6$, no. 15), *b* axis unique].[34] The nonstandard body-centered space groups were chosen in order to obtain a $\beta$ angle reasonably close to 90°. The choice of the centrosymmetric space group, *I*2/*c*, suggested by the statistics of the normalized structure factor magnitudes $|E|$,[35] was later verified by the successful refinement of the determined structure. Its solution required the location of (a) the 3 iron atoms of the cation, 1 antimony atom, 4 chlorine atoms (*viz.*, 1 of the cation, 2 of the anion, and one of the solvated $CH_2Cl_2$ molecule), 6 oxygen atoms, 21 carbon atoms, and ideally 16 hydrogen atoms each occupying the following general eightfold set of positions; (0, 0, 0; $^1/_2$, $^1/_2$, $^1/_2$) ± ($x$, $y$, $z$; $x$, $-y$, $^1/_2 + z$), and (b) the iron atom of the anion and the carbon atom of the $CH_2Cl_2$ molecule each occupying the following set of fourfold special positions on twofold axes: (0, 0, 0; $^1/_2$, $^1/_2$, $^1/_2$) ± (0, $y$, $^1/_4$).

**Determination of the Structure.** The structure was solved by the Hauptman–Karle symbolic addition method.[36] The computer program FAME[37] was first used to generate a Wilson plot from a total of 2828 observed and unobserved reflections; this plot provided both the initial scale factor and an overall isotropic temperature factor, from which the observed structure amplitudes were placed on an absolute scale, and normalized structure factor magnitudes $|E|$ were determined. Their statistical averages[35] of $\langle|E|\rangle$ = 0.781, $\langle|E|^2\rangle$ = 0.988, and $\langle|E^2 - 1|\rangle$ = 0.949, which was calculated from the initially presumed empirical composition $Sb_8Fe_{32}Cl_{40}O_{48}C_{168}$ (*vs.* the structurally found composition $Sb_8Fe_{28}Cl_{32}O_{48}C_{112}$) for each unit cell, suggest a centrosymmetric space group, in this case *I*2/*c*.

In order to use the program MAGIC,[37] this space group was transformed to *A*2/*a* by the following relations: $h_A = l_I$, $k_A = k_I$, and $l_A = -h_I - l_I$. In order to initiate the symbolic addition procedure, the origin was fixed by an assignment of positive phases to the two reflections ($\bar{9}$, 0, 13) and (5, 6, 0) of large $|E|$ magnitudes, 3.15 and 2.82, respectively. Two other reflections (*viz.*, ($\bar{8}$, 10, 8) with $|E|$ = 3.06 and (1, 9, 5) with $|E|$ = 3.31) were assigned letter phases A and B, respectively. A total of 345 reflections, each with $|E| \geq 1.50$, was used in the application of the Hauptman–Karle $\sigma$-2 relationship.[36,37] Only signs with a probability factor of $P \geq 0.99$ were accepted. After several cycles, 321 symbolic signs were determined. By then, it seemed obvious that the two letter symbols A and B must have the same sign.

A computed three-dimensional Fourier synthesis, based on the combination A = B = +, revealed initial positions for one antimony, four iron, and two chlorine atoms, the coordinates of which were transformed to coordinates based on the initial unit cell of *I*2/*c* symmetry. One cycle of full-matrix least-squares refinement of these seven atoms with individual isotropic temperature factors was carried out with a local version of the Busing–Martin–Levy ORFLS program.[38] This refinement based on the minimization of $\Sigma w_i \Delta F_i^2$ with the weights assigned according to the relationship $w_i = 1/\sigma_i^2(F_o)$, yielded $R_1 = [\Sigma(|F_o| - |F_c|)/\Sigma|F_o|] \times 100 = 32.2\%$ and $R_2 = [\Sigma w(|F_o| - |F_c|)^2/\Sigma w|F_o|^2]^{1/2} \times 100 = 39.4\%$. After two successive Fourier syntheses all nonhydrogen atoms were located including those of a solvated $CH_2Cl_2$ molecule, which was established on the basis of the positions and relative peak heights of the chlorine and carbon atoms. The discrepancy factors at this point were $R_1$ = 11.4% and $R_2$ = 11.0%. Four cycles of least-squares refinement were carried out with anisotropic thermal parameters for the antimony, iron, and chlorine atoms and isotropic ones for

(26) T. C. Furnas, Jr., "Single Crystal Orienter Instruction Manual," General Electric Co., Milwaukee, Wis., 1966.
(27) A. S. Foust, Ph.D. Thesis (Appendix), University of Wisconsin (Madison), 1970.
(28) Argonne National Laboratory, "Orientation and Angle Setting Generation Program," Program B-101, 1965.
(29) V. A. Uchtman and L. F. Dahl, *J. Amer. Chem. Soc.*, **91**, 3756 (1969).
(30) "International Tables for X-Ray Crystallography," Vol. III, Kynoch Press, Birmingham, England, 1962, p 157.
(31) J. F. Blount, DEAR, an absorption correction program based on the methods of W. R. Busing and H. A. Levy, *Acta Crystallogr.*, 10, 180 (1957).
(32) H. P. Hanson, F. Herman, J. D. Lea, and S. Skillman, *ibid.*, 17, 1040 (1964).
(33) Reference 30, p 213.
(34) Reference 30, Vol. I, 2nd ed, 1965, p 101.
(35) (a) G. H. Stout and L. H. Jensen, "X-Ray Structure Determination," Macmillan, New York, N. Y., 1968, p 321; (b) I. L. Karle, K. S. Dragonette, and S. A. Brenner, *Acta Crystallogr.*, **19**, 713 (1965).
(36) (a) H. Hauptman and J. Karle, "Solution of the Phase Problem. I. The Centrosymmetric Crystal," American Crystallographic Association Monograph No. 3, Polycrystal Book Service, Pittsburgh, Pa., 1953; (b) *cf.* I. L. Karle and J. Karle, *Acta Crystallogr.*, **16**, 969 (1963).
(37) R. B. K. Dewar and A. L. Stone, "Fame and Magic, Fortran Computer Programs for Use in the Symbolic Addition Method," University of Chicago, 1966; *cf.* E. B. Fleischer, R. B. K. Dewar, and A. L. Stone, Abstracts of Papers, American Crystallographic Association, Winter Meeting, Atlanta, Ga., 1967, p 20.
(38) W. R. Busing, K. O. Martin, and H. A. Levy, "ORFLS, A Fortran Crystallographic Least-Squares Program," ORNL-TM-305, Oak Ridge National Laboratory, Oak Ridge, Tenn., 1963.

Table II, Final Atomic Parameters with Estimated Standard Deviations

| Atom | $x$ | $y$ | $z$ | $B$, Å$^2$ |
|---|---|---|---|---|
| Sb | 0.2033 (1) | 0.2042 (1) | −0.0585 (1) | *a* |
| Fe(1) | 0.0874 (1) | 0.1450 (1) | −0.1024 (1) | *a* |
| Fe(2) | 0.3089 (1) | 0.1159 (1) | −0.0679 (1) | *a* |
| Fe(3) | 0.2127 (1) | 0.2993 (1) | 0.0572 (1) | *a* |
| Fe(4) | 0.0000 | 0.1564 (2) | 0.2500 | *a* |
| Cl(1) | 0.2119 (2) | 0.2963 (3) | −0.1648 (2) | *a* |
| Cl(2) | 0.0918 (2) | 0.0784 (2) | 0.2253 (3) | *a* |
| Cl(3) | 0.0366 (2) | 0.2397 (3) | 0.3532 (3) | *a* |
| Cl(4) | 0.0655 (5) | 0.4679 (5) | 0.2962 (5) | *a* |
| O(1) | 0.1260 (7) | 0.1273 (7) | −0.2636 (8) | 6.3 (3) |
| O(2) | 0.0329 (7) | 0.2963 (9) | −0.1415 (8) | 7.3 (3) |
| O(3) | 0.2376 (8) | 0.0118 (9) | −0.1774 (10) | 9.0 (4) |
| O(4) | 0.2761 (7) | 0.0334 (8) | 0.0746 (9) | 7.5 (3) |
| O(5) | 0.1005 (8) | 0.3961 (9) | −0.0069 (9) | 8.2 (4) |
| O(6) | 0.3195 (7) | 0.3859 (7) | −0.0159 (7) | 6.0 (3) |
| C(1) | 0.1120 (9) | 0.1349 (10) | −0.1986 (11) | 4.9 (4) |
| C(2) | 0.0548 (9) | 0.2354 (12) | −0.1240 (10) | 5.2 (4) |
| C(3) | 0.0986 (9) | 0.0630 (11) | −0.0066 (11) | 5.5 (4) |
| C(4) | 0.0806 (9) | 0.0226 (10) | −0.0814 (10) | 5.1 (4) |
| C(5) | 0.0150 (9) | 0.0533 (10) | −0.1117 (10) | 4.8 (4) |
| C(6) | −0.0060 (10) | 0.1109 (12) | −0.0564 (12) | 6.6 (5) |
| C(7) | 0.0473 (9) | 0.1164 (11) | 0.0064 (10) | 5.2 (4) |
| C(8) | 0.2642 (11) | 0.0568 (13) | −0.1316 (13) | 7.3 (5) |
| C(9) | 0.2871 (10) | 0.0654 (11) | 0.0151 (12) | 6.1 (5) |
| C(10) | 0.3647 (9) | 0.2081 (11) | −0.1151 (11) | 5.1 (4) |
| C(11) | 0.3786 (10) | 0.1361 (11) | −0.1524 (11) | 5.5 (4) |
| C(12) | 0.4085 (9) | 0.0839 (11) | −0.0956 (11) | 5.6 (4) |
| C(13) | 0.4115 (11) | 0.1220 (12) | −0.0222 (12) | 6.9 (5) |
| C(14) | 0.3851 (10) | 0.1991 (12) | −0.0345 (11) | 6.1 (5) |
| C(15) | 0.1472 (11) | 0.3529 (12) | 0.0172 (11) | 6.1 (5) |
| C(16) | 0.2750 (9) | 0.3525 (10) | 0.0122 (10) | 4.7 (4) |
| C(17) | 0.2060 (9) | 0.2014 (10) | 0.1348 (10) | 4.6 (4) |
| C(18) | 0.1590 (9) | 0.2619 (10) | 0.1527 (10) | 4.8 (4) |
| C(19) | 0.1979 (9) | 0.3337 (10) | 0.1748 (10) | 5.0 (4) |
| C(20) | 0.2664 (9) | 0.3153 (10) | 0.1679 (10) | 4.5 (4) |
| C(21) | 0.2749 (9) | 0.2351 (10) | 0.1427 (10) | 4.8 (4) |
| C(22) | 0.0000 | 0.4073 (22) | 0.2500 | 10.5 (10) |

[a] Anisotropic temperature factors of the form $\exp\{-[B_{11}h^2 + B_{22}k^2 + B_{33}l^2 + 2B_{12}hk + 2B_{13}hl + 2B_{23}kl]\}$ were used for the antimony, iron, and chlorine atoms; the resulting thermal coefficients ($\times 10^5$), with standard deviations of the last significant figure given in parentheses, are as follows.

| | $B_{11}$ | $B_{22}$ | $B_{33}$ | $B_{12}$ | $B_{13}$ | $B_{23}$ |
|---|---|---|---|---|---|---|
| Sb | 155 (4) | 235 (5) | 238 (5) | −33 (4) | −7 (3) | 1 (4) |
| Fe(1) | 161 (8) | 270 (11) | 282 (10) | −25 (7) | −11 (7) | −6 (8) |
| Fe(2) | 168 (8) | 320 (12) | 398 (11) | 1 (7) | −32 (7) | −34 (9) |
| Fe(3) | 217 (8) | 330 (11) | 271 (10) | −60 (8) | 3 (7) | −33 (9) |
| Fe(4)[b] | 171 (11) | 340 (16) | 264 (14) | 0 | −10 (10) | 0 |
| Cl(1) | 290 (16) | 438 (22) | 322 (19) | −62 (16) | 29 (14) | 91 (17) |
| Cl(2) | 174 (14) | 321 (21) | 469 (21) | 17 (13) | 40 (14) | 3 (17) |
| Cl(3) | 346 (18) | 570 (26) | 361 (21) | −108 (17) | −48 (15) | −118 (18) |
| Cl(4) | 927 (39) | 918 (45) | 993 (44) | −288 (34) | −95 (33) | 108 (36) |

[b] The location of Fe(4) on a twofold rotation axis in the *b* direction requires the anisotropic thermal coefficients $B_{12}$ and $B_{23}$ to be zero by symmetry.

the oxygen and carbon atoms. For this full-matrix anisotropic refinement, the location of the iron atom of the anion on the twofold axis requires the anisotropic thermal coefficients $B_{12}$ and $B_{23}$ to be zero by symmetry. Correction of the antimony, iron, and chlorine scattering factors for anomalous dispersion effects were made at this time, and the refinement continued for two more cycles. The final discrepancy values were $R_1 = 7.1$ and $R_2 = 6.4\%$. During the last cycle no parameter changed by more than $0.2\sigma$. A final three-dimensional Fourier difference map based on the anisotropic–isotropic refinement showed nothing unusual. No attempt was made to identify the hydrogen atoms of the cyclopentadienyl rings. All Fourier summations were computed with the Blount program.[39]

The positional and thermal parameters obtained from the output of the last cycle of the anisotropic–isotropic least-squares refinement are presented in Table II.[40] Interatomic distances and bond angles together with estimated standard deviations, calculated with the Busing–Martin–Levy function and error program[41] from the full inverse matrix (containing estimated uncertainties in lattice parameters), are listed in Tables III and IV. Equations of least-squares planes determined by a least-squares method[42] along with distances of atoms from these planes and angles between the normals of these planes are given in Table V.

Both uncorrected and thermally corrected values are given in Table III for the Sb–Fe and Sb–Cl bond lengths of the cation and for the Fe–Cl bond lengths of the anion. The particular model utilized to calculate these bond lengths over thermal motion assumes

(39) J. F. Blount, Ph.D. Thesis (Appendix), University of Wisconsin (Madison), 1965.

(40) Calculated and observed structure factors for $\{[Fe(h^5\text{-}C_6H_5)(CO)_2]_3SbCl\}_2[FeCl_4]\cdot CH_2Cl_2$ are deposited as Document No. NAPS-01332 with the ASIS National Auxiliary Publication Service, c/o CCM Information Corp., 909 3rd Ave., New York, N. Y. 10022. A copy may be secured by citing the document number and remitting $2.00 for microfiche or $5.00 for photocopies. Advance payment is required. Make checks or money orders payable to: CCMIC-NAPS.

(41) W. R. Busing, K. O. Martin, and H. A. Levy, "OR FFE, A Fortran Crystallographic Function and Error Program," ORNL-TM-306, Oak Ridge National Laboratory, Oak Ridge, Tenn., 1964.

(42) D. L. Smith, "A Least-Squares Planes Program," Ph.D. Thesis (Appendix IV), University of Wisconsin (Madison), 1962.

Table III. Interatomic Distances with Estimated Standard Deviations[a]

A. Bonding Distances (Å) in the $\{[Fe(h^5\text{-}C_5H_5)(CO)_2]_3SbCl\}^+$ Cation

| | | | |
|---|---|---|---|
| Sb–Fe(1) | 2.525 (3) | Fe(2)–C(10) | 2.10 (2) |
| | 2.527 (3)[b] | Fe(2)–C(11) | 2.06 (2) |
| Sb–Fe(2) | 2.556 (3) | Fe(2)–C(12) | 2.09 (2) |
| | 2.563 (3)[b] | Fe(2)–C(13) | 2.08 (2) |
| Sb–Fe(3) | 2.535 (3) | Fe(2)–C(14) | 2.10 (2) |
| | 2.540 (3)[b] | | 2.09 (av) |
| Sb–Cl(1) | 2.401 (4) | C(10)–C(11) | 1.42 (2) |
| | 2.414 (4)[b] | C(11)–C(12) | 1.40 (2) |
| Fe(1)–C(1) | 1.73 (2) | C(12)–C(13) | 1.40 (2) |
| Fe(1)–C(2) | 1.70 (2) | C(13)–C(14) | 1.42 (2) |
| C(1)–O(1) | 1.15 (2) | C(14)–C(10) | 1.40 (2) |
| C(2)–O(2) | 1.16 (2) | | 1.41 (av) |
| Fe(1)–C(3) | 2.14 (2) | Fe(3)–C(15) | 1.67 (2) |
| Fe(1)–C(4) | 2.13 (2) | Fe(3)–C(16) | 1.73 (2) |
| Fe(1)–C(5) | 2.10 (2) | C(15)–O(5) | 1.21 (2) |
| Fe(1)–C(6) | 2.10 (2) | C(16)–O(6) | 1.16 (2) |
| Fe(1)–C(7) | 2.10 (2) | Fe(3)–C(17) | 2.14 (2) |
| | 2.11 (av) | Fe(3)–C(18) | 2.08 (2) |
| C(3)–C(4) | 1.46 (2) | Fe(3)–C(19) | 2.11 (2) |
| C(4)–C(5) | 1.43 (2) | Fe(3)–C(20) | 2.09 (2) |
| C(5)–C(6) | 1.44 (2) | Fe(3)–C(21) | 2.12 (2) |
| C(6)–C(7) | 1.43 (2) | | 2.11 (av) |
| C(7)–C(3) | 1.39 (2) | C(17)–C(18) | 1.43 (2) |
| | 1.43 (av) | C(18)–C(19) | 1.48 (2) |
| Fe(2)–C(8) | 1.67 (2) | C(19)–C(20) | 1.38 (2) |
| Fe(2)–C(9) | 1.72 (2) | C(20)–C(21) | 1.45 (2) |
| C(8)–O(3) | 1.18 (2) | C(21)–C(17) | 1.45 (2) |
| C(9)–O(4) | 1.17 (2) | | 1.44 (av) |

B. Bonding Distances (Å) in the $FeCl_4^{2-}$ Anion

| | | | |
|---|---|---|---|
| Fe(4)–Cl(2) | 2.284 (4) | Fe(4)–Cl(3) | 2.320 (5) |
| | 2.291 (5)[b] | | 2.338 (5)[b] |

C. Bonding Distance (Å) in the $CH_2Cl_2$ Molecule

| | |
|---|---|
| C(22)–Cl(4) | 1.78 (2) |

D. Important Nonbonding Distances, Å

| | | | |
|---|---|---|---|
| Sb···O(1) | 3.90 (1) | Cl(1)···O(1) | 3.68 (1) |
| Sb···O(2) | 3.83 (1) | Cl(1)···O(2) | 3.52 (1) |
| Sb···O(3) | 3.93 (2) | Cl(1)···O(5) | 3.93 (2) |
| Sb···O(4) | 3.89 (1) | Cl(1)···O(6) | 3.50 (1) |
| Sb···O(5) | 3.97 (2) | Cl(1)···C(1) | 3.40 (2) |
| Sb···O(6) | 3.87 (1) | Cl(1)···C(2) | 3.33 (2) |
| Sb···C(1) | 3.08 (2) | Cl(1)···C(15) | 3.53 (2) |
| Sb···C(2) | 3.05 (2) | Cl(1)···C(16) | 3.29 (2) |
| Sb···C(8) | 3.08 (2) | Cl(1)···C(8) | 4.25 (2) |
| Sb···C(9) | 3.09 (2) | Cl(1)···C(10) | 3.37 (2) |
| Sb···C(15) | 3.08 (2) | Cl(1)···C(11) | 4.23 (2) |
| Sb···C(16) | 3.09 (2) | Cl(1)···C(14) | 4.22 (2) |
| Sb···C(3) | 3.31 (2) | C(1)···Cl(1″) | 3.68 (1) |
| Sb···C(4) | 3.91 (2) | Cl(2)···Cl(3) | 3.71 (1) |
| Sb···C(7) | 3.61 (2) | Cl(2)···Cl(2′)[c] | 3.71 (1) |
| Sb···C(10) | 3.33 (2) | Cl(2)···Cl(3′)[c] | 3.88 (1) |
| Sb···C(14) | 3.52 (2) | Cl(3)···Cl(3′)[c] | 3.66 (1) |
| Sb···C(17) | 3.25 (2) | Cl(4)···Cl(4′)[c] | 2.88 (1) |
| Sb···C(18) | 3.85 (2) | Cl(1)···C(2) | 2.44 (3) |
| Sb···C(21) | 3.61 (2) | C(8)···C(9) | 2.48 (3) |
| Fe(1)···Fe(2) | 4.32 (1) | C(15)···C(16) | 2.48 (3) |
| Fe(1)···Fe(3) | 4.38 (1) | | |
| Fe(2)···Fe(3) | 4.28 (1) | | |
| Fe(1)···Cl(1) | 3.74 (1) | | |
| Fe(2)···Cl(1) | 3.91 (1) | | |
| Fe(3)···Cl(1) | 3.74 (1) | | |
| Fe(1)···O(1) | 2.88 (1) | | |
| Fe(1)···O(2) | 2.85 (2) | | |
| Fe(2)···O(3) | 2.85 (2) | | |
| Fe(2)···O(4) | 2.89 (2) | | |
| Fe(3)···O(5) | 2.88 (2) | | |
| Fe(3)···O(6) | 2.89 (1) | | |
| Fe(4)···C(22) | 4.29 (4) | | |

[a] Standard deviations of the last significant figures are given in parentheses. [b] These values correspond to interatomic distances averaged over thermal motion based on a model[41] in which the second atom is assumed to ride on the first atom. [c] The chlorine atoms related to Cl(*n*) by the crystallographic twofold axis located at $x = 0$, $z = 1/4$ are designated by Cl(*n*′); the chlorine atom related to Cl(1) by a center of symmetry located at $1/4, 1/4, -1/4$ is denoted by Cl(1″).

the second atom to ride on the first one.[41] Table III shows that this model leads to increases of the uncorrected distances in the cation by less than 0.01 Å (<3σ) for the Sb–Fe bonds and by 0.013 Å (~3.3σ) for the Sb–Cl bond, and in the anion by 0.007 Å (~1.8σ) and 0.018 Å (~3.6σ) in the two crystallographically independent Fe–Cl bonds. The fact that these selected bond length changes are all less than 0.02 Å is indicative that the actual effect of anisotropic atomic thermal motion on the bond lengths and angles of both the cation and anion is not large. Furthermore, it is felt that this extreme "piggy-back riding" thermal model does not adequately represent the actual physical situation (especially that in the cation), and hence the preferred distances are those with no thermal correction.

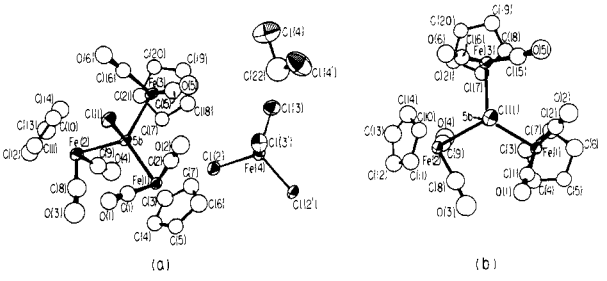

Figure 1. A general view in the crystal of $\{[Fe(h^5\text{-}C_5H_5)(CO)_2]_3SbCl\}_2[FeCl_4]\cdot CH_2Cl_2$ giving the configurations of one $\{[Fe(h^5\text{-}C_5H_5)(CO)_2]_3SbCl\}^+$ cation, one $[FeCl_4]^{2-}$ anion, and one $CH_2Cl_2$ solvent molecule; the latter two species are located on the same crystallographic twofold axis. The view at the right shows a projection of the cation down the normal to the plane containing the three iron atoms. This view clearly reveals the rotation of the one $[Fe(h^5\text{-}C_5H_5)(CO)_2]$ fragment about the Sb–Fe(2) bond by 143° relative to the dispositions of the other two $[Fe(h^5\text{-}C_5H_5)(CO)_2]$ fragments which possess essentially identical orientations with respect to the Sb–Cl bond direction. All atoms are represented by thermal ellipsoids which are scaled to the 40% probability level.

## Results and Discussion

**General Description of the Crystal Structure.** Crystalline $\{[Fe(h^5\text{-}C_5H_5)(CO)_2]_3SbCl\}_2[FeCl_4]\cdot CH_2Cl_2$ is constructed of discrete $\{[Fe(h^5\text{-}C_5H_5)(CO)_2]_3SbCl\}^+$ cations, $[FeCl_4]^{2-}$ anions, and methylene chloride molecules. Figure 1 displays the configurations of the one independent cation possessing no crystallographic constraints and those of the anion and $CH_2Cl_2$ molecule each situated on a crystallographic twofold axis. Figure 2 shows the arrangement of the eight cations, four anions, and four $CH_2Cl_2$ molecules in the centrosymmetric monoclinic unit cell. The packing is observed to be largely dominated by the bulky $\{[Fe(h^5\text{-}C_5H_5)(CO)_2]_3SbCl\}^+$ cations with the shortest interionic distances among the cations being 3.2 Å for the carbonyl oxygen···oxygen contacts, 3.3 Å for the cyclopentadienyl carbon···carbon separations, 3.7 Å for the chlorine···chlorine contacts, 3.2 Å for the oxygen···carbon separations, 3.7 Å for the oxygen···chlorine contacts, and 3.6 Å for the carbon···chlorine separations. The

Table IV. Bond Angles with Estimated Standard Deviations (Deg)[a]

| | | | |
|---|---|---|---|
| A. | $\{[Fe(h^5\text{-}C_5H_5)(CO)_2]_3SbCl\}^+$ Cation | | |
| Fe(1)-Sb-Fe(2) | 116.3 (1) | C(3)-C(4)-C(5) | 106.6 (15) |
| Fe(1)-Sb-Fe(3) | 119.8 (1) | C(4)-C(5)-C(6) | 107.8 (16) |
| Fe(2)-Sb-Fe(3) | 114.4 (1) | C(5)-C(6)-C(7) | 107.6 (17) |
| | 116.8 (av) | C(6)-C(7)-C(3) | 109.3 (17) |
| | | C(7)-C(3)-C(4) | 108.7 (16) |
| Fe(1)-Sb-Cl(1) | 98.8 (1) | | 108.0 (av) |
| Fe(2)-Sb-Cl(1) | 104.1 (1) | | |
| Fe(3)-Sb-Cl(1) | 98.5 (1) | C(10)-C(11)-C(12) | 109.4 (16) |
| | 100.5 (av) | C(11)-C(12)-C(13) | 107.3 (17) |
| | | C(12)-C(13)-C(14) | 108.1 (18) |
| Sb-Fe(1)-C(1) | 91.0 (5) | C(13)-C(14)-C(10) | 108.5 (17) |
| Sb-Fe(1)-C(2) | 90.3 (6) | C(14)-C(10)-C(11) | 106.6 (16) |
| | | | 108.0 (av) |
| C(1)-Fe(1)-C(2) | 90.8 (8) | | |
| Sb-Fe(2)-C(8) | 91.0 (7) | C(17)-C(18)-C(19) | 109.7 (15) |
| Sb-Fe(2)-C(9) | 90.2 (6) | C(18)-C(19)-C(20) | 105.4 (15) |
| C(8)-Fe(2)-C(9) | 94.1 (10) | C(19)-C(20)-C(21) | 111.8 (15) |
| Sb-Fe(3)-C(15) | 91.8 (6) | C(20)-C(21)-C(17) | 106.3 (15) |
| Sb-Fe(3)-C(16) | 90.9 (6) | C(21)-C(17)-C(18) | 106.8 (15) |
| C(15)-Fe(3)-C(16) | 93.9 (9) | | 108.0 (av) |
| Fe(1)-C(1)-O(1) | 177.5 (16) | | |
| Fe(1)-C(2)-O(2) | 177.5 (17) | | |
| Fe(2)-C(8)-O(3) | 174.6 (20) | | |
| Fe(2)-C(9)-O(4) | 175.3 (17) | | |
| Fe(3)-C(15)-O(5) | 174.8 (17) | | |
| Fe(3)-C(16)-O(6) | 176.5 (16) | | |

| | |
|---|---|
| B. $[FeCl_4]^{2-}$ Anion | |
| Cl(2)-Fe(4)-Cl(3) | 107.2 (2) |
| Cl(2)-Fe(4)-Cl(2′) | 108.5 (2) |
| Cl(2)-Fe(4)-Cl(3′) | 115.0 (2) |
| Cl(3)-Fe(4)-Cl(3′) | 104.2 (3) |
| C. $CH_2Cl_2$ Molecule | |
| Cl(4)-C(22)-Cl(4′) | 108.5 (20) |

[a] Standard deviations of last significant figures are given in parentheses.

interionic (cation carbon)···(anion chlorine) and (cation oxygen)···(anion chlorine) distances are all greater than 3.5 Å. The shortest contact distances from the solvent chlorine atoms are 3.6 Å to the carbonyl oxygen atoms, 4.0 Å to the cyclopentadienyl carbon atoms, and 4.0 Å to the anion chlorine atoms.

**The $\{[Fe(h^5\text{-}C_5H_5)(CO)_2]_3SbCl\}^+$ Cation. (a) Geometry.** In this triiron–antimony cluster system the chlorine atom and three iron atoms are bonded to the central antimony atom in a severely distorted tetrahedral arrangement. The average Fe–Sb bond length of 2.54 Å is the first such distance reported; the Sb–Cl bond length is 2.401 (4) Å. The three Fe–Sb–Fe bond angles of average value of 117° are expectedly wider than the regular tetrahedral angle of 109° 28′, while the three Fe–Sb–Cl bond angles of average value 100° are less. Figure 1 reveals that the entire cation would possess a pseudo-$C_3$-3 geometry (with the threefold rotation axis coincident with the Sb–Cl bond) if one of the three $[Fe(h^5\text{-}C_5H_5)(CO)_2]$ fragments (identified by the Fe(2) labeling) were not markedly different in orientation from those of the other two fragments by a rotation of approximately 143° about the Fe(2)–Sb axis. This radical departure of the cation from a hypothetical $C_3$-3 propeller-like arrangement of the $[Fe(h^5\text{-}C_5H_5)(CO)_2]$ fragments about the central Sb–Cl hub gives rise to a concomitant distortion of the $Fe_3SbCl$ cluster from noncrystallographic trigonal $C_{3v}$-3$m$ symmetry to $C_s$-$m$ symmetry with the remaining mirror plane passing through the Fe(2), Sb, and Cl atoms and bisecting

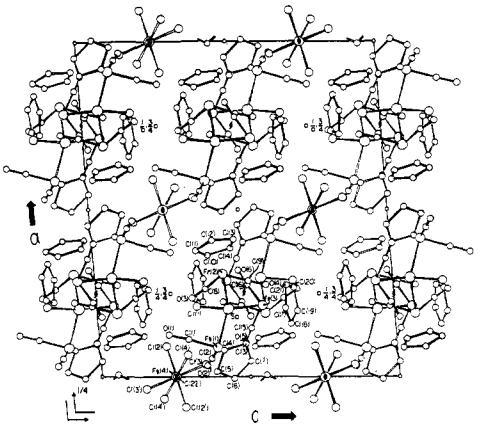

Figure 2. An [010] projection of the monoclinic unit cell of symmetry $I2/c$ showing the orientations of the four $\{[Fe(h^5\text{-}C_5H_5)(CO)_2]_3SbCl\}_2[FeCl_4]\cdot CH_2Cl_2$ species per cell. Species with solid lines connecting the atoms are situated above those with open lines connecting the atoms.

the internuclear line between the nonbonding Fe(1) and Fe(3) atoms. This distortion may be described in terms of an angular-like movement of Fe(2) on the mirror plane away from the Cl atom toward the midpoint of Fe(1) and Fe(3), as manifested both from the

Table V. Equations of "Best" Least-Squares Planes, Distances of Atoms from These Planes, and Angles between the Normals of These Planes[a,b]

| | | | |
|---|---|---|---|
| I. Equations of Planes and Distances (Å) of Selected Atoms from These Planes | | | |
| (A) Plane through Fe(1), Fe(2), and Fe(3) $0.177X + 0.624Y - 0.761Z - 3.180 = 0$ | | | |
| Sb | 0.46 | Cl(1) | 2.85 |
| (B) Plane through C(3), C(4), C(5), C(6), and C(7) $0.506X + 0.702Y - 0.501Z - 1.792 = 0$ | | | |
| Sb | 3.18 | C(3) | −0.01 |
| Cl(1) | 5.33 | C(4) | 0.00 |
| Fe(1) | 1.73 | C(5) | 0.00 |
| Fe(2) | 3.24 | C(6) | −0.01 |
| Fe(3) | 3.37 | C(7) | 0.01 |
| (C) Plane through C(10), C(11), C(12), C(13), and C(14) $0.928X + 0.332Y - 0.168Z - 8.184 = 0$ | | | |
| Sb | 3.14 | C(10) | 0.00 |
| Cl(1) | 2.05 | C(11) | 0.01 |
| Fe(1) | 5.39 | C(12) | −0.01 |
| Fe(2) | 1.71 | C(13) | 0.01 |
| Fe(3) | 2.89 | C(14) | 0.00 |
| (D) Plane through C(17), C(18), C(19), C(20), and C(21) $-0.015X + 0.286Y - 0.958Z + 1.231 = 0$ | | | |
| Sb | 3.11 | C(17) | −0.01 |
| Cl | 5.27 | C(18) | 0.01 |
| Fe(1) | 3.56 | C(19) | 0.00 |
| Fe(2) | 2.80 | C(20) | 0.00 |
| Fe(3) | 1.72 | C(21) | 0.01 |
| II. Angles (Deg) between Normals to Planes | | | |
| A and B | 24.6 | B and C | 141.9 |
| A and C | 120.0 | B and D | 47.7 |
| A and D | 25.2 | C and D | 104.0 |
| III. Angles (Deg) between Sb-Cl(1) Axis with Normals to Planes | | | |
| Sb-Cl(1) and A | 3.8 | Sb-Cl(1) and C | 117.2 |
| Sb-Cl(1) and B | 26.4 | Sb-Cl(1) and D | 26.0 |

[a] The equations of the planes are given in an orthogonal ångström coordinate system ($X$, $Y$, $Z$) which is related to the monoclinic fractional unit cell coordinate system ($x$, $y$, $z$) by the transformation $X = ax + cz \cos\beta$, $Y = by$, and $Z = cz \sin\beta$. [b] Unit weights were used for all atoms in the application of the Smith least-squares planes program.[42]

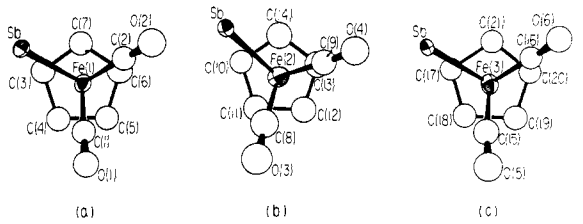

Figure 3. Local environment about each of the three crystallographically independent iron atoms of the $\{[Fe(h^5\text{-}C_5H_5)(CO)_2]_3SbCl\}^+$ cation projected normal to the cyclopentadienyl rings (for which hydrogen atoms are omitted). For both Fe(1) and Fe(3) the antimony atom and the two carbonyl groups have essentially identical orientations relative to the cyclopentadienyl ring; although the antimony and the two carbonyl ligands coordinated to Fe(2) are slightly twisted relative to the orientation of the cyclopentadienyl ring, the overall local site symmetry is remarkably similar at each of the three iron atoms.

larger Fe(2)–Sb–Cl angle of 104.1 (1)° compared to the mirror-equivalent Fe(1)–Sb–Cl and Fe(3)–Sb–Cl angles of 98.8 (1) and 98.5 (1)°, respectively, and from the resulting smaller Fe(2)-Sb–Fe(1) and Fe(2)–Sb–Fe(3) angles of 116.3 (1) and 114.4 (1)°, respectively, compared to the Fe(1)–Sb–Fe(3) angle of 119.8 (1)°. This angular deformation of the $Fe_3SbCl$ cluster is also evidenced by the nonbonding Fe(2)···Cl distance of 3.91 (1) Å being considerably greater than the chemically equivalent nonbonding Fe(1)···Cl and Fe(3)···Cl distances of common value of 3.74 (1) Å; there is also an expected smaller decrease in the nonbonding Fe(2)···Fe(1) and Fe(2)···Fe(3) distances of 4.32 (1) Å and 4.28 (1) Å, respectively, compared to the nonbonding Fe(1)···Fe(3) distance of 4.38 (1) Å. This angular deformation of the $Fe_3SbCl$ cluster can be ascribed to steric compression effects. Despite the different orientation of the one $[Fe(h^5\text{-}C_5H_5)(CO)_2]$ fragment involving Fe(2), all six nonbonding Sb···C(carbonyl) distances of 3.05–3.09 Å are very similar to one another, as also are the shortest nonbonding Sb···C(cyclopentadienyl) distances in each of the cyclopentadienyl rings of 3.31 (2), 3.33 (2), and 3.25 (2) Å, respectively. The two Cl···C(carbonyl) contacts are 3.40 (2) and 3.33 (2) Å for Fe(1) and 3.53 (2) and 3.29 (2) Å for Fe(3), while for Fe(2) there is one close nonbonding Cl···C(cyclopentadienyl) separation of 3.37 (2) Å, with the next three separations being 4.22 (2)–4.25 (2) Å.

The different orientation about the SbCl part of the cation of the one $[Fe(h^5\text{-}C_5H_5)(CO)_2]$ fragment has a noticeable yet relatively slight influence on the localized environment of the cyclopentadienyl ring, two carbonyl groups, and the antimony atom about Fe(2) compared to that of the corresponding ligands about Fe(1) and Fe(3). Figure 3 clearly shows for Fe(2) in contrast to Fe(1) and Fe(3) a slight rotation of the cyclopentadienyl ring about the Fe–(ring centroid) axis relative to the trigonal-like disposition of the antimony and two carbonyl ligands about each iron atom. However, the most notable structural feature observed in Figure 3 is the analogous geometry for each of the three $[Fe(h^5\text{-}C_5H_5)(CO)_2]$ fragments. The six Sb–Fe–CO bond angles vary from only 90.2 (6) to 91.8 (6)°, while the three OC–Fe–CO bond angles are 90.8 (8), 94.1 (10), and 93.9 (9)°. Hence, each iron atom may be considered to exhibit an approximate octahedral-like environment with the cyclopentadienyl ring functioning as a tridentate ligand.

No significant differences in the bonding of each iron atom to the cyclopentadienyl and carbonyl ligands are observed in the three $[Fe(h^5\text{-}C_5H_5)(CO)_2]$ fragments. Within limits of experimental error, each of the three cyclopentadienyl rings is a regular pentagon of average side of 1.43 Å; Table V shows that each of the five carbon atoms per ring is within 0.01 Å of the "best" least-squares plane, while the perpendicular distance of the iron atom from its attached cyclopentadienyl ring varies only from 1.71 to 1.73 Å. The Fe–C(cyclopentadienyl) distances are essentially the same in the three fragments with an average value of 2.10 Å. The six Fe–C(carbonyl) bond lengths span from 1.67 (2) to 1.73 (2) Å, with the mean value of 1.72 Å being at the longer end of the regular range observed in $[Fe(h^5\text{-}C_5H_5)(CO)_2]$ fragments in other complexes.[6b,10b,c,12,13,16] The mean value for the six C–O bond lengths is 1.17 Å, while the average nonbonding Fe···O distance is 2.87 Å as commonly observed in other iron carbonyl complexes. The Fe–C–O bond lengths do not deviate appreciably from linearity, with the average angular deviation being only 4.0°. This expected occurrence of bent Fe–C–O groups for an $Fe(CO)_2$ system can be rationalized as a composite consequence of both crystal-packing forces and electronic effects involving the different extents of utilization of the two nondegenerate $\pi_{CO}$ and two nondegenerate $\pi^*_{CO}$ orbitals in their bonding with the appropriate iron orbitals.

The simplicity of the infrared carbonyl stretching pattern of $\{[Fe(h^5\text{-}C_5H_5)(CO)_2]_3SbCl\}_2[FeCl_4]\cdot CH_2Cl_2$ in solution and its complexity in the solid state suggest that the cation may undergo a conformational change on dissolution to give actual $C_3$-3 symmetry.[43]

**(b) Stereochemical and Bonding Relationships with Tin–(Transition Metal) Complexes.** Compounds of general formula $[Fe(h^5\text{-}C_5H_5)(CO)_2L]X$ (where L is a tertiary stibine and X a large anion) can be prepared from $Fe(h^5\text{-}C_5H_5)(CO)_2Cl$ by the reaction with the stibines.[22] In salts such as $[Fe(h^5\text{-}C_5H_5)(CO)_2Sb(C_6H_5)_3]_2[PtCl_6]$, the $Sb(C_6H_5)_3$ ligand can be viewed in two extreme ways—either (1) as a noncharged ligand which forms a coordinate-covalent $\sigma$ bond with the iron atom of the positively charged $[Fe(h^5\text{-}C_5H_5)(CO)_2]$ fragment (with the antimony atom formally an Sb(V) and with the iron atom considered to be in the oxidation state 2+ if the positive charge is localized on it), analogous to the positively charged $[Fe(h^5\text{-}C_5H_5)(CO)_3]^+$ cation in the tetraphenyl borate salt $[Fe(h^5\text{-}C_5H_5)(CO)_3][B(C_6H_5)_4]$,[22] or (2) as an authentic monocharged stibonium cation (analogous to the tetraphenyl stibonium cation in the perchlorate salt $[Sb(C_6H_5)_4]ClO_4$[44]), which forms an electron pair covalent $\sigma$ bond with the iron atom of the neutral $[Fe(h^5\text{-}C_5H_5)(CO)_2]$ fragment (for which the antimony and iron atoms again may be considered to be Sb(V) and Fe(II), respectively). One can expect that the actual electronic structure of the $[Fe(h^5\text{-}C_5H_5)(CO)_2Sb(C_6H_5)_3]^+$ cation lies somewhere between the two

(43) The authors wish to acknowledge one of the referees for suggesting that the more complex solid-state infrared spectrum may be showing the effects of intermolecular coupling which necessitates the use of a crystallographic factor-group analysis; *cf.* H. J. Buttery, G. Keeling, S. F. A. Kettle, I. Paul, and P. J. Stamper, *J. Chem. Soc. A*, 471 (1970), and references cited therein.

(44) G. G. Long, J. G. Stevens, R. J. Tullbane, and L. H. Bowen, *J. Amer. Chem. Soc.*, **92**, 4230 (1970).

Table VI, Comparison of Bond Lengths and Angles of the $Fe_3SbCl$ Cluster System in the $\{[Fe(h^5\text{-}C_5H_5)(CO)_2]_3SbCl\}^+$ Cation with Those of Related Tin Complexes

| No. | Compound | A-Cl, Å[a] | A-M, Å[a] | Cl-A-Cl, deg | Cl-A-M, deg | M-A-M, deg | Ref |
|---|---|---|---|---|---|---|---|
| I | $SnCl_4$ | 2.31 (2) | | 109.4 | | | *b* |
| II | $[Fe(h^5\text{-}C_5H_5)(CO)_2]SnCl_3$ | 2.358 (6) | 2.466 (2) | 98.3 (1) | 119.2 (1) | | *c* |
| III | $[Fe(h^5\text{-}C_5H_5)(CO)_2]_2SnCl_2$ | 2.43 (1) | 2.492 (8) | 94.1 (6) | 107.2 (av) | 128.6 (3) | *d* |
| IV | $[Fe(h^5\text{-}C_5H_5)(CO)_2]_2[Mo(h^5\text{-}C_5H_5)(CO)_3]SnCl$ | 2.50 (1) | 2.590 (av) | | 102.3 (av) | 115.6 (2) | *e* |
| | | | | | 98.4 (3)[f] | 116.8 (av)[g] | |
| V | $\{[Fe(h^5\text{-}C_5H_5)(CO)_2]_3SbCl\}^+$ | 2.401 (4) | 2.54 (av) | | 100.5 (av) | 116.8 (av) | *h* |
| VI | $[Mn(CO)_5]_3SnCl$ | 2.432 (8) | 2.74 (av) | | 101.0 (av) | 116.5 (av) | *i* |

[a] A = Sn or Sb; M = Fe or Mn. [b] R. L. Livingston and C. N. R. Rao, *J. Chem. Phys.*, **30**, 339 (1959). [c] Reference 17. [d] Reference 12. [e] Reference 13. [f] M = Mo. [g] Fe-Sn-Mo angle. [h] This work. [i] Reference 14.

above-mentioned models near that of the isoelectronic neutral iron–tin species $Fe(h^5\text{-}C_5H_5)(CO)_2Sn(C_6H_5)_3$,[6b] which, on the basis of a $^{119m}Sn$ Mössbauer spectral examination has been regarded by Fenton and Zuckerman[45] as a derivative of Sn(IV).

By the same reasoning the $\{[Fe(h^5\text{-}C_5H_5)(CO)_2]_3SbCl\}^+$ cation may be considered in one sense as a trimetal-substituted derivative of the tetrachlorostibonium cation $[SbCl_4]^+$. Although this latter cation (which is isoelectronic with neutral $SnCl_4$) has not been isolated to date in the solid state, the existence of the $\{[Fe(h^5\text{-}C_5H_5)(CO)_2]_3SbCl\}^+$ cation may be ascribed to the three bulky $[Fe(h^5\text{-}C_5H_5)(CO)_2]$ ligands which effectively prevent the formation of higher coordination polyhedra about the antimony atom.

Although the Fe–Sn bond lengths are still shorter than the sum of 2.63 Å of the iron and tin covalent radii,[46] one interesting stereochemical aspect of the series of complexes $[Fe(h^5\text{-}C_5H_5)(CO)_2]_nSnCl_{4-n}$ ($n$ = 0–3) listed in Table VI is an enlargement of both the Fe–Sn and Cl–Sn bond lengths upon increased substitution of $[Fe(h^5\text{-}C_5H_5)(CO)_2]$ ligands in place of chlorine atoms (corresponding to an increase in $n$). Another consequence associated with increased coordination with $[Fe(h^5\text{-}C_5H_5)(CO)_2]$ ligands is a compensatory angular distortion about the tin atom in order to permit the Fe–Sn–Fe bond angles to be as great as possible. In the $[Fe(h^5\text{-}C_5H_5)(CO)_2]_2SnX_2$ complexes (X = Cl (no. III),[12] ONO,[10b] or $CH_3$[10c]) the Fe–Sn–Fe bond angles range from 123 to 129°,[47] while in $[Fe(h^5\text{-}C_5H_5)(CO)_2]_2[Mo(h^5\text{-}C_5H_5)(CO)_3]SnCl$ (no. IV),[13] $[Mn(CO)_5]_3SnCl$ (no. VI),[14] and the $\{[Fe(h^5\text{-}C_5H_5)(CO)_2]_3SbCl\}^+$ cation (no. V) containing three metal atoms M coordinated either to a tin or antimony atom designated as A, the M–A–M bond angle has uniformly decreased to approximately 117°. At the same time there is a concomitant diminution of the Cl–A–Fe bond angles from 119° in $[Fe(h^5\text{-}C_5H_5)(CO)_2]SnCl_3$ (no. II)[17] to 107° in $[Fe(h^5\text{-}C_5H_5)(CO)_2]_2SnCl_2$ (no. III)[12] to 101° in both the $\{[Fe(h^5\text{-}C_5H_5)(CO)_2]_3SbCl\}^+$ cation (no. V) and $[Mn(CO)_5]_3SnCl$ (no. VI).[14] A simultaneous reduction is observed in the Cl–Sn–Cl bond angle from the regular tetrahedral angle of 109° 28′ in $SnCl_4$ (no. I) to 98.3° in $[Fe(h^5\text{-}C_5H_5)(CO)_2]SnCl_3$ (no. II)[17] to 94.1° in $[Fe(h^5\text{-}C_5H_5)(CO)_2]_2SnCl_2$ (no. III).[12]

Although these above correlations concerning bond lengths and angular distortions from a normal tetrahedral environment about the tin atom in these complexes are dictated *at least* partially by steric hindrance effects, various bonding explanations have been advanced to account for the observed trends as $[Fe(h^5\text{-}C_5H_5)(CO)_2]$ fragments are substituted in place of chlorine atoms (corresponding to an increase of $n$ in the above series). One proposal essentially is based on the invoking of a directional $\sigma$-bond effect involving enhanced s-orbital character in each Sn–Fe bond concomitant with a concentration of p-orbital character in each Sn–Cl bond.[12,48] These trends can also be rationalized primarily in terms of decreased $d\pi$(Fe)–$d\pi$(Sn) interactions on the premise that it can be expected that the tin atom is in a more reduced state such that its orbitals become higher in energy relative to those of each $[Fe(h^5\text{-}C_5H_5)(CO)_2]$ fragment; hence, the $d\pi$(Fe)–$d\pi$(Sn) interaction per $[Fe(h^5\text{-}C_5H_5)(CO)_2]$ fragment should be less as $n$ increases.[49] This bonding model also appears to be coherent from the viewpoint that as $n$ increases the amount of $\pi$-type electron charge accumulated by the $SnCl_{4-n}$ fragment from *each* of the $n$ $[Fe(h^5\text{-}C_5H_5)(CO)_2]$ ligands would be expectedly less in accord with a weaker Fe–Sn bond as evidenced by a longer Fe–Sn bond length. It is noteworthy that the degree and importance of $d\pi$–$d\pi$ bonding between transition metals and ligands of main group IVb and Vb elements have been widely debated in the literature,[48,50–55] and

(45) D. E. Fenton and J. J. Zuckerman, *Inorg. Chem.*, **8**, 1771 (1969).
(46) L. Pauling, "The Nature of the Chemical Bond," 3rd ed, Cornell University Press, 1960; (a) p 246; (b) p 260.
(47) Another indication that steric effects dictate the nature of the angular distortion from a tetrahedral environment about the tin atom is shown from the X-ray study[16] of $[Fe(h^5\text{-}C_5H_5)(CO)_2]_2Sn(h^1\text{-}C_5H_5)_2$ which revealed an Fe–Sn–Fe angle of only 115.9°; this smaller angle than those found in the other $[Fe(h^5\text{-}C_5H_5)(CO)_2]_2SnX_2$ complexes is attributed to the more bulky $\sigma$-bonded $C_5H_5$ ligands.
(48) D. E. Fenton and J. J. Zuckerman, *J. Amer. Chem. Soc.*, **90**, 6226 (1968).
(49) Even in the absence of detailed MO calculations, it is proper to conclude that the most important atomic orbitals which contribute to any $\pi$-bonding character of Cl–A and Fe–A bonds (where A represents Sn or Sb) are the filled $3p\pi$ orbitals of each Cl atom, the filled $3d\pi$ orbitals of each Fe atom, and the vacant $5d\pi$ orbitals of the Sn or Sb atom. On the basis of a consideration of the relative energies of these orbitals which are reasonably presumed to be $3p\pi(Cl) < 3d\pi(Fe) < 5d\pi$, it is concluded that any $3d\pi$(Fe)–$5d\pi$(Sn or Sb) back-bonding must be of much greater importance than *any* $3p\pi$(Cl)–$5d\pi$(Sn or Sb) back-bonding.
(50) An extensive compilation of references dealing with a discussion of $d\pi$–$d\pi$ bonding in (transition metal)–(main group IVb) compounds is cited by Fenton and Zuckerman[48] in a footnote (ref 4).
(51) An excellent review of recent theoretical and experimental evidence for the participation of outer d orbitals in bonding has been written by K. A. R. Mitchell, *Chem. Rev.*, **69**, 157 (1969).
(52) S. O. Grim and D. A. Wheatland, *Inorg. Chem.*, **8**, 1716 (1969); H. J. Plastas, J. M. Stewart, and S. O. Grim, *J. Amer. Chem. Soc.*, **91**, 4326 (1969), and references contained therein.
(53) R. J. Angelici and C. M. Ingemanson, *Inorg. Chem.*, **8**, 83 (1969), and references cited therein.
(54) L. M. Venanzi, *Chem. Brit.*, **4**, 162 (1968).
(55) R. E. Dessy and L. Wieczorek, *J. Amer. Chem. Soc.*, **91**, 4963 (1969), and references contained therein.

definite stands have been taken on the basis of $^{119m}Sn$ Mössbauer and nmr proton data against such $\pi$-bonding interactions in these Sn–Fe complexes.[48,56]

The $\{[Fe(h^5\text{-}C_5H_5)(CO)_2]_3SbCl\}^+$ cation appears appropriate as an operational test of whether the $\pi$-bonding rationale has a predominant influence on the stereochemistry of these systems. As the result of the increased positive charge (and consequently greater electronegativity) on the Sb(V) atom relative to that on the Sn(IV) atom in the neutral isoelectronic $[Fe(h^5\text{-}C_5H_5)(CO)_2]_3SnCl$ analog, the empty 5d orbitals of the antimony atom are contracted and have lower energies more suitable for increased $d\pi(Fe)$–$d\pi(Sb)$ bonding.[49] To the extent that such a $\pi$ interaction alone plays the dominant role in making the Fe–Sb bond stronger, it would normally be expected that there would be an appreciable reduction in the Fe–Sb bond lengths compared to the Fe–Sn bond lengths.

Although the structure of the isoelectronic $[Fe(h^5\text{-}C_5H_5)(CO)_2]_3SnCl$ molecule has not yet been reported, the geometry of the electronically equivalent $[Fe(h^5\text{-}C_5H_5)(CO)_2]_2[Mo(h^5\text{-}C_5H_5)(CO)_3]SnCl$ molecule (no. IV in Table VI) is known.[13] Because these two complexes formally differ only by the substitution of one of the three $[Fe(h^5\text{-}C_5H_5)(CO)_2]$ fragments with a $[Mo(h^5\text{-}C_5H_5)(CO)_3]$ one, a comparison of the distances between the corresponding Cl–Sb and Cl–Sn bonds and between the corresponding Fe–Sb and Fe–Sn bonds is informative. On the basis of the estimated change of 0.04 Å in the tetrahedral covalent radii of Sn (1.40 Å)[46a] and Sb (1.36 Å)[46a] together with the determined difference of 0.10 Å between the Cl–Sn bond length of 2.50 (1) Å and the Cl–Sb bond length of 2.401 (4) Å, the relative shrinking of the tetrahedral-like covalent radius of Sb in the Cl–Sb bond is about 0.06 Å. This contraction may be attributed to a coupling of two interdependent factors: (1) the more compact size of the antimony orbitals owing to the localization of a significant fraction of the positive charge on the antimony atom and (2) *greater* covalency in the Cl–Sb $\sigma$ bond than in the Cl–Sn one owing to the appropriate orbitals of the more positively charged (and hence more electronegative) antimony system being energetically nearer to the 3s and 3p chlorine orbitals than those of the corresponding tin system.

In the neutral molecular complex $[Mn(CO)_5]_3SnCl$ (no. VI of Table VI),[14] where both the Cl–Sn–Mn and Mn–Sn–Mn bond angles are almost identical with the corresponding Cl–Sb–Fe and Fe–Sb–Fe angles in the $\{[Fe(h^5\text{-}C_5H_5)(CO)_2]_3SbCl\}^+$ cation, the close agreement between the Cl–Sn bond length of 2.432 (1) Å and the Cl–Sb bond length of 2.401 (4) Å (after allowance for the Sb radius being 0.04 Å shorter than the Sn radius) suggests that the Sn atom in $[Mn(CO)_5]_3SnCl$ has a similar fractional positive charge as that of the Sb atom in the $\{[Fe(h^5\text{-}C_5H_5)(CO)_2]_3SbCl\}^+$ cation owing to the much greater electron-withdrawing capabilities of the $[Mn(CO)_5]$ ligands.

Whereas the Sb–Cl and Sn–Cl bond lengths differ from each other by 0.10 Å, the average Fe–Sb bond length of 2.54 Å in the cation is only 0.05 Å shorter than the average Fe–Sn bond length of 2.59 Å in the electronically equivalent $Fe_2MoSnCl$ system, thereby signifying (in light of the 0.04-Å radii difference between Sn and Sb) that the electronic distributions in these Sb–Fe and Sn–Fe bonds are not dissimilar. The same average value of 117° for the Fe–Sb–Fe and Fe–Sn–Fe bond angles provides support for this hypothesis. This relative bond-length shortening can only be viewed at best qualitatively, because the Cl–Sn and Cl–Sb bond lengths can be affected by the different Cl–Sn–Fe and Cl–Sb–Fe bond angles (Table VI) as well as by concomitant steric effects due to the size difference between the $[Mo(h^5\text{-}C_5H_5)(CO)_3]$ and $[Fe(h^5\text{-}C_5H_5)(CO)_2]$ ligands (*vide infra*). Nevertheless, this lack of significant reduction in the observed Sb–Fe bonds compared to the observed Sn–Fe bonds after correction for the radii difference of Sb and Sn supports the premise that $3d\pi(Fe)$–$5d\pi(Sn \text{ or } Sb)$ bonding does not appear to play a major role in determining the physical and chemical properties of these compounds. This conclusion is not incompatible with the infrared data of the complexes listed in Table VII. If the infrared carbonyl stretching frequencies are deemed as a sensitive indicator for a qualitative estimation of any relative differences in partial charge transfer from the iron atom,[57,59] as can be seen in the first four entries in Table VII, which show for the isoelectronic complexes that the corresponding carbonyl frequencies increase about 400 $cm^{-1}$ with the increment of four formal oxidation state units on the metal atoms, then the similarity of the infrared spectral data of the Sb and Sn systems given in Table VII shows that in these complexes the iron atoms are at almost the

Table VII. Comparison of Carbonyl Stretching Frequencies of the $\{[Fe(h^5\text{-}C_5H_5)(CO)_2]_3SbCl^+\}$ Cation with Those of Other Complexes Containing $[Fe(h^5\text{-}C_5H_5)(CO)_2]$ Groups

| Species | C–O stretching frequencies, $cm^{-1}$ | Ref |
|---|---|---|
| $[V(h^5\text{-}C_5H_5)(CO)_3]^{2-}$ | 1748 (vs), 1645 (vs) | *a* |
| $[Cr(h^5\text{-}C_5H_5)(CO)_3]^-$ | 1876 (vs), 1695 (vs) | *a* |
| $[Mn(h^5\text{-}C_5H_5)(CO)_3]$ | 2035 (vs), 1953 (vs) | *a* |
| $[Fe(h^5\text{-}C_5H_5)(CO)_3]^+$ | 2120 (vs), 2070 (vs) | *b* |
| $[Fe(h^5\text{-}C_5H_5)(CO)_2Sb(C_6H_5)_3]^+$ | 2050 (vs), 2005 (vs) | *b* |
| $[Fe(h^5\text{-}C_5H_5)(CO)_2As(C_6H_5)_3]^+$ | 2062 (vs), 2017 (vs) | *b* |
| $[Fe(h^5\text{-}C_5H_5)(CO)_2P(C_6H_5)_3]^+$ | 2070 (vs), 2030 (vs) | *b* |
| $Fe(h^5\text{-}C_5H_5)(CO)_2CN$ | 2060 (vs), 2020 (vs) | *c* |
| $Fe(h^5\text{-}C_5H_5)(CO)_2Cl$ | 2050 (vs), 2010 (vs) | *c* |
| $Fe(h^5\text{-}C_5H_5)(CO)_2CH_3$ | 2010 (vs), 1955 (vs) | *d* |
| $Fe(h^5\text{-}C_5H_5)(CO)_2C_2H_5$ | 2010 (vs), 1950 (vs) | *d* |
| $Fe(h^5\text{-}C_5H_5)(CO)_2(C_6H_5)$ | 2020 (vs), 1960 (vs), 1930 (m) | *d* |
| $Fe(h^5\text{-}C_5H_5)(CO)_2(h^1\text{-}C_5H_5)$ | 2013 (vs), 1965 (vs) | *d* |
| $\{[Fe(h^5\text{-}C_5H_5)(CO)_2]_3SbCl\}^+$ | 2050 (sh), 2025 (vs), 1990 (vs) | This work |
| $[Fe(h^5\text{-}C_5H_5)(CO)_2]_2SnCl_2$ | 2040 (sh), 2025 (vs), 1993 (vs) | *e* |
| $Fe(h^5\text{-}C_5H_5)(CO)_2SnCl_3$ | 2062 (vs), 1980 (vs) | *e* |

[a] R. D. Fischer, *Chem. Ber.*, **93**, 165 (1960). [b] Reference 22. [c] T. S. Piper, F. A. Cotton, and G. Wilkinson, *J. Inorg. Nucl. Chem.*, **1**, 165 (1955). [d] T. S. Piper and G. Wilkinson, *ibid.*, **3**, 104 (1956). [e] F. Bonati and G. Wilkinson, *J. Chem. Soc.*, 179 (1964).

(56) V. I. Goldanskii, E. F. Makarov, and R. A. Stukan, *J. Chem. Phys.*, 47, 4048 (1967).

(57) In the isoelectronic series $[V(CO)_6]^-$ (1859 $cm^{-1}$), $Cr(CO)_6$ (1981 $cm^{-1}$), and $[Mn(CO)_6]^+$ (2101 $cm^{-1}$),[58] the MO calculations of Caulton and Fenske[59] indicate that the effective charge on the central metal atom decreases by 0.72 electron from the $[V(CO)_6]^-$ anion to neutral $Cr(CO)_6$ and by 0.56 electron from $Cr(CO)_6$ to the $[Mn(CO)_6]^+$ cation.

(58) R. W. Cattrall and R. J. H. Clark, *J. Organometal. Chem.*, **6**, 167 (1966).

(59) K. G. Caulton and R. F. Fenske, *Inorg. Chem.*, 7, 1273 (1968).

same effective oxidation state and are in a much more reduced state than the one in the $[Fe(h^5\text{-}C_5H_5)(CO)_3]^+$ cation. The similarity of the spectra of the $\{[Fe(h^5\text{-}C_5H_5)(CO)_2]_3SbCl\}^+$ cation and the $[Fe(h^5\text{-}C_5H_5)(CO)_2]_2SnCl_2$ molecule supports the premise that there is no detectable difference in the relative charge density localized on the iron atoms in these complexes, and hence the difference between $d\pi$(Fe)–$d\pi$(Sb) and $d\pi$(Fe)–$d\pi$(Sn) back-bonding (coupled with any difference in the synergistic $\sigma$ bonding) is not appreciable.

The much larger difference of 0.10 Å between the Sb–Cl and Sn–Cl bond lengths compared to the difference of 0.05 Å between the Fe–Sb and Fe–Sn bond lengths may intuitively be ascribed to the more ionic Cl–Sb or Cl–Sn bonds being much more sensitive to the electronegativity differences between the antimony and tin systems (as reflected in the formal oxidation states Sn(IV) and Sb(V) in these complexes) than the more covalent Fe–Sb and Fe–Sn bonds.

**Stereochemistry and Bonding of the $[FeCl_4]^{2-}$ Anion.** Although the $[FeCl_4]^{2-}$ anion has been extensively characterized by Mössbauer, magnetic susceptibility, electronic, and far-infrared spectral studies,[23,60] at the time this investigation was carried out no detailed crystallographic information concerning its bond lengths was available. The existence of this anion as a regular tetrahedral species in the crystalline bis(triphenylmethylarsonium) tetrachloroferrate(II) salt was implied by Pauling,[61] who demonstrated from unit cell parameter data that crystals of this compound and of corresponding compounds containing other $[MCl_4]^{2-}$ anions (M = Mn, Co, and Zn) are isomorphous with those of $[As(C_6H_5)_3(CH_3)]_2[NiCl_4]$, which he showed from a three-dimensional X-ray structural analysis to have the $[NiCl_4]^{2-}$ anion in a regularly tetrahedral configuration within experimental error.

The $[MCl_4]^{2-}$ anions are known to form charge-transfer complexes with other molecules.[62–65] A charge-transfer effect occurs in a number of salts of the paraquat cation, the doubly charged ion of *N*,*N*′-dimethyl-4,4′-dipyridylium (abbreviated $pq^{2+}$), with tetrahalogenometalate anions including the $[FeCl_4]^{2-}$ one.[62,63] X-Ray powder patterns indicate that the structure of $pqFeCl_4$ is very similar to that of $pqCoCl_4$ whose structure was completely elucidated from an X-ray diffraction analysis;[62,63a] it is noteworthy that esr spectra of the tetrachloroferrate(II) salt show[63b] that this solid contains some of the reduced radical cation and some oxidized anion. Two independent preliminary reports[64a,b] of the crystallographic characterization of the bis(3,5-dimethyl-1,2-dithiolylium) tetrachloroferrate(II) salt, $(C_5H_7S_2)_2FeCl_4$, have provided unequivocal evidence that each tetrahedral $[FeCl_4]^{2-}$ anion forms a crystalline charge-transfer complex[64c] by the use of all four chlorine atoms which make a total of six short contacts with the sulfur atoms of four surrounding dithiolylium cations. The resulting $[FeCl_4]^{2-}$ anion possesses crystallographic $C_2$-2 site symmetry with the two independent Fe–Cl bond lengths from one study[64a] being 2.289 (5) and 2.335 (5) Å and from the other investigation[64b] being 2.31 (1) and 2.34 (1) Å; the angles subtended at the iron atom by the pairs of symmetry-related chlorine atoms were reported in both studies[64a,b] to be 112 and 116°. However, prior to this investigation, it was not possible to estimate the extent of Fe–Cl bond-length elongation due to the charge-transfer interactions in the $(C_5H_7S_2)_2FeCl_4$ complex. It is now shown that the average value for the Fe–Cl bond lengths in this complex is not appreciably longer than that found for the $[FeCl_4]^{2-}$ anion in the $\{[Fe(h^5\text{-}C_5H_5)(CO)_2]_3SbCl\}_2[FeCl_4]\cdot CH_2Cl_2$ salt.

The tetrachloroferrate(II) anion in the $\{[Fe(h^5\text{-}C_5H_5)(CO)_2]_3SbCl\}_2[FeCl_4]\cdot CH_2Cl_2$ salt also deviates significantly from $T_d$-$\bar{4}3m$ cubic symmetry. As observed in other tetrachlorometalate complexes of the first-row transition metals,[66] the $[FeCl_4]^{2-}$ anion has the form of a flattened tetrahedron with two Cl–Fe–Cl angles larger (with identical values of 115.0 (2)°) and four Cl–Fe–Cl angles smaller (with one value of 104.2 (3)°, two values of 107.2 (2)°, and one value of 108.5 (2)°) than the ideal tetrahedral angle (Table VIII). The Cl(2)–Fe–Cl(2′) plane is also twisted approximately 6° around the twofold crystallographic axis passing through the iron atom relative to the Cl(3)–Fe–Cl(3′) plane. Although at a first glance this distortion may be ascribed partially to a Jahn–Teller effect, because in a regular high-spin tetrahedral environment $Fe^{2+}(d^6)$ has the electronic configuration $e^3(2t_2)^3$ with three electrons in the doubly degenerate e orbitals,[67] other complexes show this same kind of tetrahedral distortion when no Jahn–Teller effect is operable, such as in the $[FeCl_4]^-$ anion,[68–70] in the $[CoCl_4]^{2-}$ anion,[66,71] and in the $[ZnCl_4]^{2-}$ anion.[66,72] Qualitative correlation of the angular distortions with specific crystal-packing effects were demonstrated in the case of $Cs_3(Cl)[CoCl_4]$.[71] Hence, it is concluded that crystal-packing forces dictated by the size and shape of the cation as well as its polarizable nature have a predominate effect on the deviations of the anion from strict tetrahedral symmetry.

The $[NiCl_4]^{2-}$ anion, which likewise may be expected to possess a Jahn–Teller type distortion, experimentally was found to possess regular tetrahedral geometry in one salt,[61] a flattened tetrahedral framework in another salt,[66] and an elongated tetrahedral framework in a third salt.[73] A large detectable Jahn–Teller distortion is considered to account for the observed deformation of the

(60) (a) R. J. H. Clark, R. S. Nyholm, and F. B. Taylor, *J. Chem. Soc. A*, 1802 (1967); (b) P. R. Edwards, C. E. Johnson, and R. J. P. Williams, *J. Chem. Phys.*, **47**, 2074 (1967); (c) G. M. Bancroft and J. M. Dubery, *ibid.*, **50**, 2264 (1969).

(61) P. Pauling, *Inorg. Chem.*, **5**, 1498 (1966).

(62) For a recent review of charge-transfer complexes, see C. K. Prout and J. D. Wright, *Angew. Chem., Int. Ed. Engl.*, **7**, 659 (1968).

(63) (a) C. K. Prout and P. Murray-Rust, *J. Chem. Soc. A*, 1520 (1969); (b) A. J. Macfarlane and R. J. P. Williams, *ibid.*, *A*, 1517 (1969).

(64) (a) R. Mason, E. D. McKenzie, G. B. Robertson, and G. A. Rusholme, *Chem. Commun.*, 1673 (1968); (b) H. C. Freeman, G. H. W. Milburn, C. E. Nockolds, P. Hemmerich, and K. H. Knauer, *ibid.*, 55 (1969); (c) G. A. Heath, R. L. Martin, and I. M. Stewart, *ibid.*, 54 (1969).

(65) A. Mostad and C. Rømming, *Acta Chem. Scand.*, 22, 1259 (1968).

(66) J. R. Wiesner, R. C. Srivastava, C. H. L. Kennard, M. DiVaira, and E. C. Lingafelter, *Acta Crystallogr.*, **23**, 565 (1967).

(67) Clark, Nyholm, and Taylor[60a] concluded that the abnormally high magnetic moments observed for the $[FeX_4]^{2-}$ anions (where X = Cl, Br, or I) when associated with a number of large cations can be plausibly explained if some contribution to the ground electronic state from the $3d^54s$ contribution is assumed.

(68) B. Zaslow and R. E. Rundle, *J. Phys. Chem.*, **61**, 490 (1957).

(69) M. J. Bennett, F. A. Cotton, and D. L. Weaver, *Acta Crystallogr.*, **23**, 581 (1967).

(70) T. J. Kistenmacher and G. D. Stucky, *Inorg. Chem.*, **7**, 2150 (1968).

(71) B. N. Figgis, M. Gerloch, and R. Mason, *Acta Crystallogr.*, **17**, 506 (1964).

(72) B. Morosin and E. C. Lingafelter, *ibid.*, **12**, 611 (1959).

(73) G. D. Stucky, J. B. Folkers, and T. J. Kistenmacher, *ibid.*, **23**, 1064 (1967).

Table VIII. Stereochemical Comparison of the $[FeCl_4]^{2-}$ Anion with Other $[MCl_4]^{2-}$ Anions (M = Mn, Co, Ni, Cu, or Zn) and with the $[FeCl_4]^{-}$ Anion

| Species | Salt | Crystallographic site symmetry of anion | M–Cl bond distance, Å (uncorr)[a] | M–Cl bond distance, Å (corr)[b] | Cl–M–Cl bond angle, deg | Shape[c] | Ref |
|---|---|---|---|---|---|---|---|
| $[MnCl_4]^{2-}$ | $[N(CH_3)_4]_2[MnCl_4]$ | $C_s$-$m$ | 2.324 (av) | 2.372 (av) | | | *d* |
| $[FeCl_4]^{2-}$ | $[C_5H_5S_2]_2[FeCl_4]$ | $C_2$-2 | [2] 2.289 (5)<br>[2] 2.335 (5)<br>2.313 (av) | | [1] 112<br>[1] 116<br>[2] 106<br>[2] 108 | F | *e* |
| | $[C_5H_5S_2]_2[FeCl_4]$ | $C_2$-2 | [2] 2.31 (1)<br>[2] 2.34 (1) | | [1] 112<br>[1] 116<br>[2] 106<br>[2] 108 | F | *f* |
| | $\{[Fe(h^5\text{-}C_5H_5)(CO)_2]_3SbCl_2\}$-$[FeCl_4]$ | $C_2$-2 | [2] 2.284 (4)<br>[2] 2.320 (5)<br>2.302 (av) | [2] 2.291 (5)<br>[2] 2.338 (5)<br>2.314 (av) | [1] 104.2 (3)<br>[1] 108.5 (2)<br>[2] 107.2 (2)<br>[2] 115.0 (2) | F | This work |
| $[CoCl_4]^{2-}$ | $[N(CH_3)_4]_2[CoCl_4]$ | $C_s$-$m$ | [1] 2.229 (9)<br>[2] 2.261 (6)<br>[1] 2.266 (9)<br>2.252 (av) | [1] 2.248<br>[2] 2.287<br>[1] 2.306<br>2.280 (av) | [2] 108.3 (2)<br>[1] 112.8 (4)<br>[2] 108.3 (2)<br>[4] 110.8 (4) | F | *g* |
| | $Cs_3(Cl)[CoCl_4]$ | $D_{2d}$-$\bar{4}2m$ | [4] 2.252 (13) | | [2] 106.1<br>[4] 111.2 | E | *h* |
| $[NiCl_4]^{2-}$ | $[N(CH_3)_4]_2[NiCl_4]$ | $C_s$-$m$ | [1] 2.220 (4)<br>[2] 2.240 (3)<br>[1] 2.234 (4)<br>2.231 (av) | [1] 2.256<br>[2] 2.279<br>[1] 2.283<br>2.273 (av) | [2] 107.8 (1)<br>[1] 114.4 (2)<br>[2] 107.8 (1)<br>[1] 111.4 (2) | F | *g* |
| | $[N(C_2H_5)_4]_2[NiCl_4]$ | $D_{2d}$-$\bar{4}2m$ | [4] 2.245 (3) | | [2] 106.83 (14)<br>[4] 110.81 (7) | E | *i* |
| | $[As(C_6H_5)_3(CH_3)]_2[NiCl_4]$ | $C_3$-3 | [3] 2.267 (8)<br>[1] 2.271 (7) | | [3] 109.3 (2)<br>[3] 109.6 (3) | R | *j* |
| $[CuCl_4]^{2-}$ | $[N(CH_3)_4]_2[CuCl_4]$ | $C_1$-1 | [1] 2.229 (3)<br>[1] 2.263 (3)<br>[1] 2.263 (2)<br>[1] 2.268 (2)<br>2.256 (av) | | [1] 100.3 (1)<br>[1] 132.1 (1)<br>[1] 99.1 (1)<br>[1] 98.3 (1)<br>[1] 132.8 (1)<br>[1] 99.7 (1) | F | *k* |
| $[ZnCl_4]^{2-}$ | $[N(CH_3)_4]_2[ZnCl_4]$ | $C_s$-$m$ | [1] 2.244 (4)<br>[2] 2.246 (3)<br>[1] 2.253 (4)<br>2.248 (av) | [1] 2.274<br>[2] 2.285<br>[1] 2.303<br>2.287 (av) | [2] 109.1 (1)<br>[1] 112.1 (2)<br>[2] 108.4 (1)<br>[1] 109.9 (2) | F | *g*, *l* |
| $[FeCl_4]^{-}$ | $[As(C_6H_5)_4][FeCl_4]$ | $S_4$-$\bar{4}$ | [4] 2.19 (3) | | [2] 114.5 (1.5)<br>[4] 107.0 (1.5) | F | *m* |
| | *trans*-$[FeCl_2(DMSO)_4][FeCl_4]$ | $S_4$-$\bar{4}$ | [4] 1.162 (5) | | [2] 112.2 (3)<br>[4] 108.1 (3) | F | *n* |
| | $[PCl_4][FeCl_4]$ | $C_s$-$m$ | [2] 2.1819 (10)<br>[1] 2.1873 (15)<br>[1] 2.1869 (14)<br>2.185 (av) | [2] 2.2077 (11)<br>[1] 2.2125 (16)<br>[1] 2.2015 (14)<br>2.207 (av) | [2] 108.98 (4)<br>[2] 108.20 (4)<br>[1] 108.83 (6)<br>[1] 113.56 (6) | I | *o* |

[a] Without correction for thermal motion. Brackets mean the number of bond distances or bond angles having the value listed in the right column. [b] With correction for thermal motion. "Riding" model[41] assumed. [c] R = essentially regular tetrahedron, F = flattened tetrahedron, E = elongated tetrahedron, I = irregularly shaped tetrahedron. [d] B. Morosin, quoted in ref 66. [e] Reference 64a. [f] Reference 64b. [g] Reference 66. [h] Reference 71. [i] Reference 73. [j] Reference 61. [k] Reference 74. [l] Reference 72. [m] Reference 68. [n] Reference 69. [o] Reference 70.

$[CuCl_4]^{2-}$ anion,[74] where the tetrahedron is so flattened that two angles are 132° while the other four angles are reduced to 100°.

In the $[FeCl_4]^{2-}$ anion the two independent Fe–Cl bond lengths are 2.284 (4) and 2.320 (5) Å; the average value of 2.30 Å bridges the gap of M–Cl bond lengths in the sequence of $[MCl_4]^{2-}$ anions (M = Mn, Fe, Co, Ni, Cu, and Zn) given in Table VIII. The Fe–Cl bond lengths corrected for anisotropic thermal motion by use of the piggy-back riding model[41] are also listed in Table VIII. These latter bond lengths do not differ appreciably (*i.e.*, only by 0.007 and 0.018 Å) from the corresponding thermally uncorrected bond lengths.

The observed trend for the M–Cl bond distances, which become shorter as the atomic number of M increases, can be rationalized on the basis of qualitative molecular orbital considerations. For a regular tetrahedron with $T_d$ symmetry the most important occupied

(74) M. Bonamico and G. Dessy, *Theor. Chim. Acta*, 7, 367 (1967); B. Morosin and E. C. Lingafelter, *J. Phys. Chem.*, 65, 50 (1961).

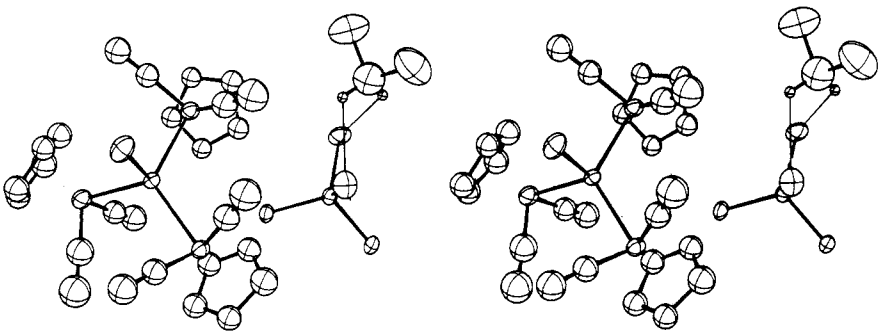

Figure 4. Stereoscopic view showing the arrangement of one $\{[Fe(h^5\text{-}C_5H_5)(CO)_2]_3SbCl\}^+$ cation with respect to the closest $[FeCl_4]^{2-}$ anion (at the lower right) and a $CH_2Cl_2$ molecule (at the upper right), both of which lie on the same crystallographic twofold axis. The hydrogen atoms attached to the cyclopentadienyl rings are omitted for clarity. The indicated C—H···Cl interactions are shown between two of the four chlorine atoms of the $[FeCl_4]^{2-}$ anion and both hydrogen atoms of the $CH_2Cl_2$ molecule. All atoms except the hydrogen atoms are represented by 40% probability ellipsoids of thermal displacement.

molecular orbitals are the bonding orbitals of $t_2$ symmetry ($1t_2$) which are mostly ligand in character, the slightly antibonding degenerate e orbital pair, and the antibonding $2t_2$ orbitals which are mainly metal in character. As the atomic number of M increases, two effects are operational. (1) The 3d orbitals of the central metal atom become closer in energy to the 3s and 3p valence orbitals of the chlorine ligands, such as to give greater $\sigma$-bond involvement of the metal atom with the four chlorine ligands; thus, the covalent bonding character of the $1t_2$ orbitals is enhanced and the bonds become shorter. (2) At the same time, more electrons are added either to the slightly antibonding e orbitals or to the antibonding $2t_2$ orbitals such that the M–Cl bonds are weakened and hence become longer. These two effects are more or less counterbalanced by each other in cases where electrons are added to the antibonding $2t_2$ orbitals, and consequently for such tetrachlorometalate anions the bond distances do not change significantly. However, if an electron is added to the e orbitals, the stabilizing effect caused by the simultaneous addition of a proton to the nucleus appears to be more important than the destabilizing effect due to the added electron, and therefore the M–Cl bonds become shorter. In the series of tetrachlorometalate complexes presented in Table VIII, from Mn(II) with electronic configuration $e^2(2t_2)^3$ (under assumed $T_d$ symmetry) to Co(II) with electronic configuration $e^4(2t_2)^3$, the M–Cl bond lengths decrease notably in accord with the addition of the electrons to the e orbitals. But from Co(II) to Zn(II) the M–Cl bond lengths remain almost constant when the electrons are added to the antibonding $2t_2$ orbitals. The above-mentioned effects can be observed separately in the two pairs $[MnCl_4]^{2-}$–$[FeCl_4]^-$ and $[FeCl_4]^-$–$[FeCl_4]^{2-}$. The isoelectronic $[MnCl_4]^{2-}$–$[FeCl_4]^-$ pair has under $T_d$ symmetry the electronic configuration $e^2(2t_2)^3$, but in the Fe(III) anion with the formal oxidation state increased by one unit it is expected that the Fe(III)–Cl bond lengths should become stronger than the Mn(II)–Cl bond lengths both because of the lower energy of the 3d iron orbitals (and hence more significant covalent interaction with the chlorine $\sigma$ orbitals) and because of the more compact iron orbital size due to the increased positive iron nuclear charge; the resulting bond stabilization then is much more important, in agreement with the Fe(III)–Cl bond length being considerably shorter by 0.14 Å. In the $[FeCl_4]^-$–$[FeCl_4]^{2-}$ pair, one extra electron in the Fe(II) anion is added to the antibonding e orbitals (under $T_d$ symmetry), and this factor combines with the size expansion of the 3d iron orbitals due to a less positive charge on the iron(II) nucleus to give an Fe(II)–Cl bond length that is approximately 0.12 Å longer than the Fe(III)–Cl one.[75]

The two crystallographically independent Fe–Cl bond distances in the $[FeCl_4]^{2-}$ anion are significantly different from each other, the difference being 0.035 ± 0.007 Å. This variation can hardly be attributed only to crystal-packing forces. An interaction involving only two of the four chlorine atoms of the $[FeCl_4]^{2-}$ anion with a $CH_2Cl_2$ molecule is discussed below to account partially for the observed variation in the two independent Fe–Cl bond lengths of 2.284 (4) and 2.320 (5) Å with the longer bond length associated with the two chlorine atoms weakly linked with the hydrogen atoms of the methylene chloride molecule.

**Stereochemical Influence of the $CH_2Cl_2$ Solvent Molecule.** In each $CH_2Cl_2$ molecule the carbon atom is located on a twofold rotation axis of the crystal lattice. The C–Cl bond length of 1.78 (2) Å agrees remarkably well with the value of 1.7724 ± 0.0005 Å obtained by microwave measurements.[76] Although the Cl–C–Cl angle of 108.5 ± 2.0° has a rather high standard deviation, this large uncertainty can be understood in terms of the excessive thermal motion of the small $CH_2Cl_2$ molecule in the crystal lattice, as seen by the high temperature factors of the C(22) and Cl(4) atoms given in Table II and by their thermal ellipsoids shown in Figures 1 and 4. This Cl–C–Cl angle is not significantly smaller than the microwave value of 111.8° determined for $CH_2Cl_2$ in the vapor phase.[76]

The hydrogen atoms of the $CH_2Cl_2$ were not located owing to the presence of relatively "heavy" antimony and iron atoms. From the C–H bond length of 1.07 Å and H–C–H bond angle of 112° determined for gaseous $CH_2Cl_2$,[76] the coordinates of the two hydrogen atoms (related to each other by a twofold crystallographic

(75) A similar observed increase of 0.18 Å occurs in the Co–N bond length of 2.114 (9) Å in the high-spin cobalt(II) hexaammine cation of the $[Co(NH_3)_6]Cl_2$ salt relative to that of 1.936 (15) Å in the low-spin cobalt(III) hexaammine cation of the $[Co(NH_3)_6]I_3$ salt: N. E. Kime and J. A. Ibers, *Acta Crystallogr., Sect. B*, 25, 168 (1969). Hence, the composite antibonding electron and orbital-size effects on the metal radii in the $[Co(NH_3)_6]^{2+}$–$[Co(NH_3)_6]^{3+}$ pair, with two unpaired electrons in the degenerate $e_g^*$ orbitals (based on assumed $O_h$ symmetry) for the octahedral-like cobalt(II) cation *vs.* none in the same antibonding orbitals for the corresponding oxidized cobalt(III) cation, appear to be similar in magnitude to those found in the $[FeCl_4]^{2-}$–$[FeCl_4]^-$ pair.

(76) R. J. Myers and W. D. Gwinn, *J. Chem. Phys.*, 20, 1420 (1952).

axis) were calculated with the aid of the program MIRAGE[77] to be the following: $x = -0.02194$, $y = 0.37230$, $z = 0.29447$; H(1'), $x = 0.02194$, $y = 0.37230$, $z = 0.20553$. Based on these coordinates, the one independent H(1)···Cl(3) distance is 2.69 Å, about 0.3 Å shorter than a normal van der Waals contact.[46b] The capability of halogenated hydrocarbon compounds in forming hydrogen bonds is well known,[78] and in our laboratories an example was found in which the interaction between the hydrogen atom of $CHCl_3$ and a sulfur atom of a $Co_4(h^5\text{-}C_5H_5)_4S_6$ molecule gave rise to distinct molecular distortions of part of the $Co_4S_6$ system.[29] The H(1)···Cl(3)–Fe(4) bond angle of 98.3° in the $\{[Fe(h^5\text{-}C_5H_5)(CO)_2]_3SbCl\}_2[FeCl_4]\cdot CH_2Cl_2$ compound is close enough to a regular tetrahedral angle to secure an interaction between a normally nonbonding electron pair from each of two chlorine atoms of the $[FeCl_4]^{2-}$ anion with the corresponding hydrogen atom of the associated $CH_2Cl_2$ molecule. This interaction should lessen the population of the $1t_2$ molecular orbitals of the $[FeCl_4]^{2-}$ anion (assumed in these bonding arguments to still conform to $T_d$ cubic symmetry) and thereby weaken the Fe–Cl bonds. The longer independent Fe(4)–Cl(3) bond length of 2.320 (5) Å relative to the independent Fe(4)–Cl(2) bond length of 2.284 (4) Å is an indication of such a bond weakening. Hence, the distortion of the $[FeCl_4]^{2-}$ anion appears to be due partially to weak hydrogen bonding of the $CH_2Cl_2$ molecule.

(77) J. Calabrese, "Program MIRAGE," Ph.D. Thesis, University of Wisconsin (Madison), 1971.

(78) G. C. Pimentel and A. L. McClellan, "The Hydrogen Bond," W. H. Freeman, San Francisco, Calif., 1959, pp 197–200.

**Acknowledgments.** This work was accomplished by the financial support of the National Science Foundation (Grant No. GP-4919). T.-T. gratefully expresses his sincere appreciation to the Agency for International Development for a predoctoral fellowship (PIO/P No. 730/90111). The use of the UNIVAC 1108 and CDC 3600 Computers at the University of Wisconsin Computing Center was made possible through partial support of the National Science Foundation and the Wisconsin Alumni Research Foundation through the University Research Committee.

# Diastereotopic Nonequivalence in Asymmetric Tin Compounds. Inversion and Halogen Exchange[1]

**Dennis V. Stynes[2] and A. L. Allred***

*Contribution from the Department of Chemistry and the Materials Research Center, Northwestern University, Evanston, Illinois 60201.* *Received August 6, 1970*

**Abstract:** The factors influencing the magnitude of diastereotopic nonequivalence in the nmr spectra of asymmetric tin compounds are discussed. A comparison of a wide variety of asymmetric tin compounds indicates that the large anisotropy of the phenyl ring is important in establishing a sufficient difference in shielding for diastereotopic nonequivalence to be observed. All three diastereotopic groups in benzylmethylneophyltin chloride are observably anisochronous in nonpolar solvents. Analysis of the coalescence of all three sets of diastereotopic peaks provides definitive evidence for a rapid inversion of configuration of the asymmetric tin center in trialkyltin halides. The concentration dependence of the mean lifetime of the asymmetric tin center indicates a second-order process. A five-coordinate halogen-bridged intermediate is proposed to explain the observed halogen exchange accompanying inversion.

The interpretation of diastereotopic nonequivalence in the nmr spectra of asymmetric molecules is complicated by a number of factors.[3] Magnetic nonequivalence arises from very subtle differences in shielding which depend on the magnetic anisotropy of all the other groups in the molecule and their orientations with respect to each of the diastereotopic nuclei. Thus the shielding differences will be influenced by any factor which changes the conformation of the molecule.[4] In addition, any molecular motion resulting in an interchange of the magnetic environments of the diastereotopic nuclei, such as an inversion of configuration, will also affect the magnitude of the observed splitting.

Recently, diastereotopic nonequivalence has been applied to organotin compounds.[5,6] Peddle and Redl[6] reported two distinct peaks for the diastereotopic methyl groups in the nmr spectrum of methylneophylphenyltin chloride (**1**). Coalescence of the signals could be produced by increasing the concentration, increasing the temperature, increasing the solvent polarity, or adding a small amount of a Lewis base. The observed line broad-

(1) (a) This research was supported in part by the Advanced Research Projects Agency of the Department of Defense, through the Northwestern University Materials Research Center; (b) presented at the 160th National Meeting of the American Chemical Society, Chicago, Ill., Sept 1970.

(2) National Institutes of Health Predoctoral Research Fellow.

(3) M. van Gorkom and G. E. Hall, *Quart. Rev., Chem. Soc.*, 22, 14 (1968).

(4) The chemical shift difference between the diastereotopic nuclei is given by the equation $\Delta_{ab} = \Delta_{cp} + \Delta_{id}$, where $\Delta_{cp}$ is a temperature-dependent contribution due to unequal conformer populations and $\Delta_{id}$ is a temperature independent contribution due to the intrinsic diastereotopic nonequivalence: M. Raban, *Tetrahedron Lett.*, 3105 (1966).

(5) (a) F. P. Boer, J. J. Flynn, H. H. Freedman, S. V. McKinley, and V. R. Sandel, *J. Amer. Chem. Soc.*, **89**, 5068 (1967); (b) F. P. Boer, G. A. Doorakian, H. H. Freedman, and S. V. McKinley, *ibid.*, **92**, 1225 (1970).

(6) G. J. D. Peddle and G. Redl, *ibid.*, **92**, 365 (1970).